SWITCHED-MODE UREA DOSING CONTROL DESIGN FOR SELECTIVE CATALYTIC REDUCTION IN A DIESEL ENGINE

A Thesis

Submitted to the Faculty

of

Purdue University

by

Rajakumar Ganne

In Partial Fulfillment of the

Requirements for the Degree

of

Master of Science in Mechanical Engineering

May 2020

Purdue University

West Lafayette, Indiana

THE PURDUE UNIVERSITY GRADUATE SCHOOL
STATEMENT OF THESIS APPROVAL

Dr. Peter H. Meckl, Chair

School of Mechanical Engineering

Dr. Gregory M. Shaver

School of Mechanical Engineering

Dr. Galen B. King

School of Mechanical Engineering

Approved by:

Dr. Nicole Key

Head of the School Graduate Program

Dedicated to my parents, brother and the protection of our planet.

ACKNOWLEDGMENTS

I am forever indebted to Dr. Peter H. Meckl, and thank him for giving me the opportunity to work on this project under his guidance and nurturing my interest in the field of controls. His patience, support and belief in me have kept me motivated. I also feel fortunate to have worked under his supervision as a TA for two different courses on Controls, which were incredible learning experiences. I thank Dr. Gregory Shaver and Dr. Galen King for being willing to serve on my advisory committee and providing valuable feedback on the thesis. Thanks also to the School of Mechanical Engineering at Purdue University for providing financial support in the form of a Teaching Assistantship.

I thank Kaushal Jain for being a patient mentor, a great friend, and for all the fun while discussing about and testing crazy ideas in simulation. Kaushal's help in understanding the SCR system and his knowledge and experience with control system design have been very helpful to me.

Most importantly, I am grateful to my family for the opportunities that they have given me and their never-ending support. It is only through my parents' guidance and support that I have found my passion for STEM. Thanks to my brother and partner-in-crime, Tagore for sharing in all my experiences. Finally, I thank my family for their unparalleled love.

TABLE OF CONTENTS

Page

LIST OF TABLES

LIST OF FIGURES

Figure Page

Figure Page

Figure Page

SYMBOLS

F	Exhaust gas volume flow rate
$\dot{m}_{DEF}$	Mass flow rate of diesel exhaust fluid
R	Universal gas constant
T	Catalyst bed temperature
u_1	Concentration of injected NH_3
u_2	Concentration of incoming NOx slip
V	Catalyst volume
x_1	Concentration of NH_3 slip
x_2	Concentration of emitted NOx
x_3	Fraction of catalyst storage capacity occupied by NH_3

ABBREVIATIONS

2WD	Two Wheel Drive
AC	Alternating Current
ADC	Analog-to-Digital Converter
AWD	All Wheel Drive
BTU	British Thermal Unit
CAN	Controller Area Network
CSTR	Continuous Stirred-Tank Reactor
DEF	Diesel Exhaust Fluid
DOC	Diesel Oxidation Catalyst
DPF	Diesel Particulate Filter
ECM	Engine Control Module
EEA	European Environment Agency
EGR	Exhaust Gas Recirculation
EPA	Environmental Protection Agency
FTP	Federal Test Procedure
HWFET	Highway Fuel Economy Test
LDV	Light-Duty Vehicles
LSO	Low Side Output
MPC	Model Predictive Control
NMOG	Non-Methane Organic Gases
PAU	Power Absorption Unit
PDE	Partial Differential Equation
PI	Proportional-Integral
PID	Proportional-Integral-Derivative
PM	Particulate Matter

PTTR	Parallel-Through-The-Road
RTD	Resistance Temperature Detector
SCR	Selective Catalytic Reduction
SNCR	Selective Non-Catalytic Reduction
SUV	Sport Utility Vehicle
UDDS	Urban Dynamometer Driving Schedule

ABSTRACT

Ganne, Rajakumar M.S.M.E., Purdue University, May 2020. Switched-Mode Urea Dosing Control Design for Selective Catalytic Reduction in a Diesel Engine. Major Professor: Peter H. Meckl, School of Mechanical Engineering.

The increasingly-stringent regulations on tailpipe NOx are difficult to meet with engine management strategies in isolation. The Urea-SCR aftertreatment system technology offers a key solution to this problem. However, the complexity of chemical reactions, strong temperature dependence of effectiveness, and the transient nature of disturbances make the system very challenging to control and offer an opportunity to develop creative control techniques.

Urea-dosing controllers developed for previous work in our research group require customization to the specific drivecycle on which they are being run. The goal of the present work is to develop controllers that are able to work on multiple drivecycles without using information specific to the drivecycle. To meet the control objective of maximizing the NOx reduction while maintaining the instantaneous concentration of gaseous ammonia at the tailpipe, referred to as NH_3 slip, under a defined ceiling, one slip-reference controller and two switched-mode controllers are proposed. The slip-reference controller consists of a model-based component which uses the observed storage fraction estimate, and a feedback component that uses only NH_3 slip information. The two switched-mode controllers switch between slip-tracking and storage-tracking mode depending on a switching logic. The first switched-mode controller uses a constant storage-reference and a temperature-dependent switching logic. The second one is designed to have predictive capability and uses a lookup-table to vary the storage-reference with time. By default, at any time, the controller is assigned the same mode as it was in the previous timestep and is changed to slip-tracking or storage-tracking when the observed storage value is either less than or

greater than the storage reference by a certain margin, respectively. Studies from simulation show the effectiveness of the three control strategies for three different drivecycles. The effects of uncertainty in model parameters, errors in urea dosing, and inaccuracies in the observer's initial conditions are also studied.

1. INTRODUCTION

As the global economy continues to grow, the demand for energy is expected to rise along with it. The transportation sector constitutes a significant fraction of this demand. Developing countries like India and China are expected to make a disproportionately high contribution to this rise in energy demand as their economies and populations continue to grow. The projected trend for energy consumption in the transportation sector is clearly illustrated in Figure 1.1.

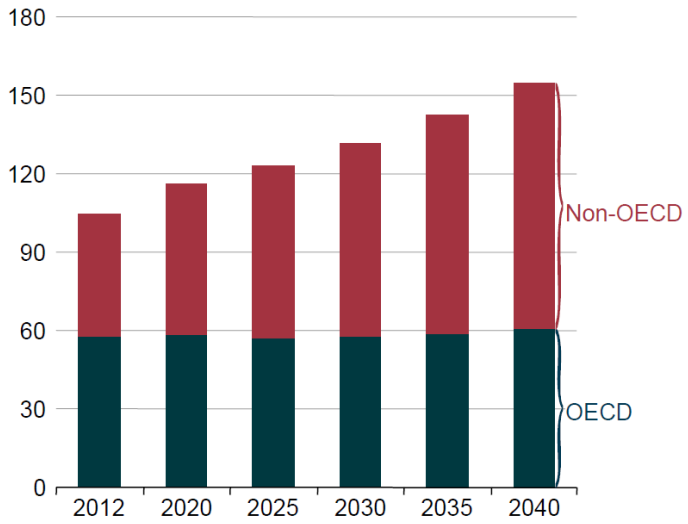

Figure 1.1. Forecast of delivered transportation energy consumption (in quadrillion BTU) by country grouping [1]

Climate change can be attributed to greenhouse gas emissions from human activity with a high degree of confidence [2]. Diesel offers multiple advantages in comparison to other fuel sources. Diesel has a high energy density and is less volatile than gasoline, thus allowing safer handling. Diesel engines are the most efficient internal combustion engines [3]. Small four-stroke direct injection turbocharged diesel engines can reach efficiencies of 40%. There are two key factors that allow for such high

efficiency in diesel engines. Diesel engines are lean-burn by design and operate at much higher compression ratios than gasoline engines, thus allowing for a higher thermal efficiency. Secondly, part-load efficiencies of diesel engines are high owing to the fact that load control is achieved by changing the air-fuel ratio, eliminating the need for throttling. The higher efficiency allows for a lower greenhouse gas footprint in comparison to other fuel sources. Despite the recent increases in electrification and hybridization of fleets, a significant proportion of vehicles are projected to have an Internal Combustion Engine, even in 2050, as evident from Table 2 of [4].

Due to their lean-burn nature (high air-to-fuel ratio), there is an excess of O_2 and N_2 present in the combustion chamber in the presence of elevated temperatures and pressures. These conditions lead to the production of NOx. NOx levels from diesel engines are higher than those from gasoline engines. The three-way catalysts used for NOx reduction in gasoline engines do not work well for diesel engines because of the oxidizing nature of the exhaust present in lean-burn engines [5] and alternative technologies such as Selective Catalytic Reduction (SCR) are required.

The present work for the control of the Urea-SCR system is done for a 2013 Chevrolet Malibu that was retrofitted with a 1.7 L diesel engine to power the front wheels and a 100 kW Magna electric motor powering the rear wheels. This vehicle is shown in Figure 1.2. The onboard energy source for the electric motor is a 16.2 kWh Li-ion battery pack.

Figure 1.2. EcoCAR2: Modified Chevrolet Malibu 2013.

1.1 Regulations for NOx and NH_3 emissions

Organizations such as the Environmental Protection Agency (EPA) in the U.S. and the European Environmental Agency (EEA) in the E.U. set regulations for various pollutants. The EPA regulations for NOx and NH_3 slip have evolved over the years. Typical limits for allowable tailpipe NH_3 slip are a mean of 10 ppm and a peak of 30 ppm [6]. Regulations for NOx from the EPA have become more stringent in various tiers. The Chevrolet Malibu being used for this study would fall under the category of Light-Duty Vehicles (LDV). The same emission standards apply to all vehicles irrespective of their fuel source.

Table 1.1. EPA regulations timeline [7].

Standard	**Adopted/Finalized on**	**Phase-in Period**
Tier 1	June 5, 1991	1994-1997
Tier 2	December 21, 1999	2004-2009
Tier 3	March 3, 2014	2017-2025

The FTP-75 drivecycle is used to test emissions from vehicles. Tier-1 regulations required the NOx emissions from passenger cars/light-duty vehicles to stay under 1.25 g/mile for the entirety of the vehicle's life (the earlier of 10 years/100,000 miles).

Tier 2 and Tier 3 regulations require companies to certify individual vehicles to any of the certification bins shown in Table 1.1, but the average NOx emission limits of 0.07 g/mile for the entire vehicle fleet need to be met [7]. Under Tier 2 regulations, vehicles of various weight classes (cars, minivans, light-duty trucks, and SUVs) have the same emission limits, which means that the vehicles with larger engines need to use more advanced technology to stay compliant. Tier 3 standards require the fleet averaged NOx+NMOG (non-methane organic gases) emissions for the vehicle fleet to be under the limit of 0.03 g/mi which is to be met by 2025 [7]. The individual vehicle regulations for the three Tiers are listed in Tables 1.2, 1.3 and 1.4.

Table 1.2. Tier 1 Regulations (g/mi for FTP-75) [8].

Time-frame	**5 yrs/50,000 miles**	**10 yrs/100,000 miles**
NOx emission limit (g/mi)	1	1.25

Table 1.3. Tier 2 Regulations (g/mi for FTP-75) [8].

Bin	**11**	**10**	**9**	**8**	**7**	**6**	**5**	**4**	**3**	**2**	**1**
5 yrs/50,000 miles	-	0.4	0.2	0.14	0.11	0.08	0.05	-	-	-	-
10 yrs/100,000 miles	0.9	0.6	0.3	0.2	0.15	0.1	0.07	0.04	0.03	0.02	0

Table 1.4. Tier 3 Regulations for NMOG+NOx (g/mi for FTP-75) [9].

Bin	**160**	**125**	**70**	**50**	**30**	**20**	**0**
15 yrs/150,000 miles	0.16	0.125	0.07	0.05	0.03	0.02	0

1.2 Diesel Engine Aftertreatment Systems

In order to meet the emission standards set by the regulatory agencies, various OEMs use in-cylinder techniques. However, there is often a tradeoff between the numerous pollutants. For instance, NOx levels can be brought down by employing Exhaust Gas Recirculation (EGR) but this comes with an increase in soot. In-cylinder techniques in isolation are therefore limited in their ability to meet emission standards. This motivates the need for using aftertreatment systems placed downstream of the engine to deal with various pollutants. Figure 1.3 shows the schematic of a typical aftertreatment system for a diesel engine. The direction of the flow of exhaust gases is from left to right in the figure. Note how the upstream NOx sensor is placed upstream of the Diesel Exhaust Fluid (DEF) injector. This is important because production NOx sensors are cross-sensitive to NH_3, which is produced from the hydrolysis and thermolysis of DEF. The aftertreatment system of the EcoCAR2

consists of a Diesel Oxidation Catalyst (DOC), a Diesel Particulate Filter (DPF) and a Selective Catalytic Reduction (SCR) system, which are discussed in this section.

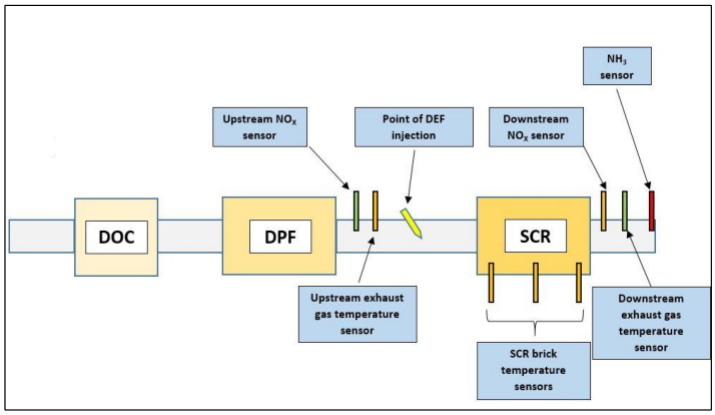

Figure 1.3. Schematic of a typical diesel engine after-treatment system [8].

1.2.1 Diesel Oxidation Catalyst (DOC)

The DOC is typically the first component of the aftertreatment system placed after the engine. Three primary functions performed by the DOC are:

1. Oxidation of CO to CO_2
2. Oxidation of partially burnt and unburnt hydrocarbons, and
3. Oxidation of NO to NO_2. The NOx in the engine-out exhaust is primarily NO. The ability of the SCR, which is located downstream of the DOC, to reduce NOx effectively is affected by the NO/NO_2 ratio at the SCR inlet and peaks when this ratio is 1. The DOC helps in oxidizing some of the NO to bring this ratio close to 1. It is important to note that the DOC does not necessarily change the total number of moles of NOx itself. It only changes the composition of the NOx.

1.2.2 Diesel Particulate Filter (DPF)

The human body cannot protect itself from particles smaller than 10 micrometer (PM-10). The DPF is a catalytic filter that helps trap the particulate matter from diesel exhaust gas. With time, the filter can get clogged up and cause significant back pressure, which consequently affects the combustion processes. To avoid such problems, the DPF needs to undergo periodic filter regeneration in which very high temperatures are realized in the DPF to oxidize the trapped particulate matter.

1.2.3 Urea-Selective Catalytic Reduction (SCR)

Various technologies such as Lean NOx traps, SCR, and Selective Non-Catalytic Reduction (SNCR) have been proposed to help achieve emission targets for NOx. Of these, SCR has been the most promising for automotive applications. In a Urea-SCR system, urea is injected into the exhaust stream which is then converted to NH_3 by means of thermolysis and hydrolysis. This NH_3 is adsorbed onto the catalyst and reduces NOx in the exhaust to produce N_2 and H_2O. The unreacted NH_3 appears at the tailpipe as slip.

1.3 Current Research

1.3.1 Motivation

Historically, Urea-SCR systems have been used in stationary applications such as power plants. For such applications where transients in the inlet conditions (NOx, flow rate, temperature) are rare, open-loop lookup-table-based control algorithms were sufficient to achieve the desired emissions targets. When the SCR technology first started being used for automotive applications, similar lookup-table-based control algorithms sufficed. As the EPA regulations have become stringent with time, real-time feedback-based control algorithms became necessary to meet these emission targets. For feedback about emissions at the tailpipe, the use of NOx sensors has

been studied widely. The major drawback of using NOx sensors is that they are cross-sensitive to NH_3 and thus give unreliable estimates. NH_3 sensors may serve as a reliable alternative and have been studied recently for NH_3-slip-based control of the SCR. Steep gradients in SCR temperature can cause sudden surges of tailpipe NH_3 slip. Further, the performance of the urea dosing control algorithm needs to be independent of the drivecycle. To solve these problems, simplified linear models of the SCR used in many studies may not suffice. Nonlinear model-based control algorithms are required.

1.3.2 Objective

The objective of this study is to develop a urea-dosing control algorithm to maximize the ability of the Urea-SCR system to reduce the concentration of NOx from the exhaust while maintaining NH_3 slip concentration under a defined upper limit (50 ppm), for a wide range of operating conditions for both transient and steady-state drivecycles. This would involve the following tasks:

1. Develop control strategies to satisfy the control objective while eliminating the need for using a NOx sensor.

2. Study the effects of model uncertainties, both structural and parametric, to assess their impact on controller performance.

3. Study the impact of urea injector faults by building errors into urea dosing by the injector.

4. Study how the performance of the NH_3 storage observer impacts controller performance.

1.3.3 Key Challenges

The SCR system, despite offering many advantages, has some key challenges that need to be addressed:

1. Nonlinearity: The chemistry of the SCR system makes it an inherently non-linear system. Many of the reactions are coupled and add a lot of complexity. Traditional control approaches that are applied to linear systems will not work with such a system.

2. Temperature Sensitivity: The Urea-SCR system is highly sensitive to temperature. There is a narrow temperature window in which the deNOx ability of the system is good.

3. Tradeoff between pollutants: The system essentially relies on the injection of one pollutant (NH_3) to minimize the other (NOx). When the concentration of either of these pollutants is low, the concentration of the other is high. Maintaining the concentrations of both within acceptable levels is challenging.

4. Disturbances: The nature of the exhaust can be very transient. The SCR system would need to work across a wide range of volumetric flow rates, temperatures, and concentrations of engine-out NOx.

5. System Lag: There is a non-zero time lag between the moments the urea is injected, the NH_3 is adsorbed onto the catalyst and is able to react with the incoming NOx.

6. Actuator limits: There is only a single degree of actuation available in the form of urea injection. Even this actuator is restricted because there is an upper limit of 28% and a lower limit of 0% on the duty cycle that can be realized.

7. Sensing challenges:

    - NOx sensing: Production NOx sensors are cross-sensitive to NH_3. This makes the NOx sensor readings unreliable whenever there is non-zero NH_3

slip. Further, this cross-sensitivity does not remain constant and is a strong function of temperature and NH_3 concentration.

- NH_3 storage measurement: It is not possible to directly measure the amount of NH_3 adsorbed onto the catalyst at any given moment. This requires the use of complicated model-based observers.

8. System Degradation: The Urea-SCR system 'ages' with time. As the system ages, its ability to catalyze key reactions and reduce NOx decreases.

1.4 Contributions

Most of the literature available, at the time of writing, for the control of Urea-SCR deals with NOx sensor-based strategies, with the control objective not always being well-defined. The primary goal of this project has been the development of NH_3 sensor based control strategies that maintain tailpipe NH_3 slip below 50 ppm, which work for multiple drivecycles. Three control strategies were developed to achieve this:

1.4.1 Controller-1: Slip-Tracking Controller

A slip-tracking controller was developed to track the desired slip-reference (50 ppm in this project). First, a model-based control component was created to leverage our knowledge of Urea-SCR system dynamics, to enable slip-reference tracking. The ammonia storage fraction that is required in this component was estimated using a real-time dynamic model-based observer developed by Jain [10]. The model-based component was appended with a PI (Proportional-Integral) feedback component to improve slip-tracking performance of the controller and to account for model uncertainty, injector errors and observer inaccuracy.

1.4.2 Controller-2: Switched Mode Controller with Temperature-based switching

A PI storage-reference tracking controller was developed. The role that temperature plays in giving rise to peaks in NH_3 slip is discussed. A switching algorithm that determines whether the controller should operate in the slip-tracking mode or the storage-tracking mode depending on the real-time catalyst bed temperature was also developed. The storage-reference is held at 2%. Simulation results show that this controller has an improved slip performance over Controller-1.

1.4.3 Controller-3: Switched Mode Controller with Ammonia Storage-Based Switching

A final switched mode controller is developed to make switching more intuitive and to minimize the number of tunable parameters. This controller has the same structure as Controller-2. The storage reference is varied with time, based on a lookup table that enables the controller to predict future NH_3 slip peaks in a receding time window. A mode-switching algorithm is developed to change controller modes depending on whether the estimated NH_3 storage value is within a certain relative upper and lower threshold of the storage reference.

Simulation results show that this controller arguably has the best performance of the three controllers. The control objective is not violated in the presence of model uncertainty, injector errors and observer inaccuracies.

1.5 Distribution of Thesis Content

This thesis consists of six chapters. Chapter 2 reviews the literature on control design for SCR systems. Chapter 3 discusses the experimental setup used by our research group to obtain experimental data related to the SCR system. Chapter 4 describes the mathematical models of the SCR system used for designing and eval-

uating the performance of the urea dosing control strategy. Chapter 5 describes the control strategies developed and the subsequent changes that were made to improve the performance of the controller. It also contains results obtained from each iteration of the controller when run on different drivecycles. Chapter 6 contains the key conclusions and lists recommendations for future work in the field.

2. LITERATURE REVIEW

The Urea-SCR aftertreatment system is quite tricky to control owing to the non-linearity of the system's dynamics, complexity of the chemical reactions, and the transient nature of disturbances that come with automotive systems. This has led to the proposal of a wide variety of control solutions over the years. What differentiates any given control strategy is the unique combination of (i) the control objective of minimizing the tailpipe NOx, NH_3 slip or a combination of both, (ii) sensor configuration for measuring concentrations of the various reacting species at the inlet and outlet of the Urea-SCR system, the temperatures of the exhaust gas stream and the catalyst brick, and flow rates, (iii) the mathematical models of the SCR system used for both offline development of control algorithms and for real-time deployment, and (iv) the control algorithm itself that is used.

This chapter reviews the literature on existing control solutions for the SCR system. Section 2.1 lists the various control objectives used in the field. Section 2.2 describes the combinations of physical sensors and observers used to obtain signals important in controlling the system. The various mathematical models used for control and plant simulation are discussed in Section 2.3. Section 2.4 describes the control laws/algorithms used in the different references.

2.1 Control Objectives

The most commonly seen control objective in the literature on SCR is to maximize NOx reduction while minimizing NH_3 slip. Several different references ([11–18]) use this objective. This is not a well-defined objective and due to the trade-off between tailpipe NH_3 slip and NOx, can seem too general. Some of these references add an extra constraint to this objective. For instance, in [11] an upper limit is placed on the

allowable urea injection rate. Similarly, [14] adds another objective of reducing the total amount of injected urea. Reference [15] attempts to keep the NH_3 slip under a specific constraint.

Reference [19] is one of the earliest sources to have a well-defined control objective. The goal in this source is to achieve a NOx reduction of at least 50% while keeping the average NH_3 slip below 10 ppm. The 50% NOx reduction is to meet the Euro IV emission requirements.

A much more advanced and well-defined control objective for the SCR is used in references [20, 21]. The objective is to minimize a modified conversion efficiency metric, which is given by:

$$\eta_T = \frac{C_{NOx,in} - C_{NOx,out} - \lambda C_{NH_3}}{C_{NOx,in}} \tag{2.1}$$

$$= \eta_{NOx} - \lambda \frac{C_{NH_3}}{C_{NOx,in}} \tag{2.2}$$

where C_i represents the concentration of species i. The goal would be to maximize this efficiency metric. From equation 2.2 the reader may note that this modified efficiency metric clearly incentivizes NOx reduction while penalizing excessive NH_3 slip for a given amount of engine-out NOx. The relative penalty on NH_3 slip can be adjusted by changing λ.

In [22], the cost function to be minimized in the Model Predictive Control Strategy was defined as:

$$J = \Sigma||y_{ref} - y||^2 + \lambda||\Delta u||^2 \tag{2.3}$$

where y_{ref} is the target NOx conversion efficiency, y is the actual NOx conversion efficiency and Δu is the change in controller effort.

2.2 Sensing Configuration

The amount of sensing used for control of Urea-SCR for automotive applications has increased with time. Quantities such as the flow rate of exhaust gases, the engine-

out NOx concentration, the catalyst bed temperature and the injected NH_3 concentration need to be known in order to control the SCR system well. Further, the stored NH_3 plays an important role in the dynamics of the system, but cannot be measured directly.

Open-loop strategies like the one presented in [13] do not require any sensors at the tailpipe because they do not use feedback. Closed-loop control strategies require some form of sensing to enable feedback. The NOx sensor is most commonly used due to its affordability. A majority of the sources like [11]- [12], [20]- [22] use tailpipe NOx sensor feedback. The drawback to using tailpipe NOx sensors is that they are cross-sensitive to any tailpipe NH_3. The cross-sensitivity also changes with temperature and ammonia concentration and is hard to model. Recently a few studies have explored using tailpipe NH_3 sensors instead. Using NH_3 sensors, the control strategy developed in [23] achieves a performance better than that of NOx-sensor based strategies.

Placing an NH_3 sensor at the SCR inlet would increase the overall system cost without adding much value. Instead, the conversion of urea to NH_3 at the inlet is modeled using a first-order lag in [12] and [24]. The variation of NH_3 concentration along the length of the SCR catalyst brick is also captured with this model. The concentration of NH_3 at the SCR inlet is given by:

$$\frac{\dot{m}_{NH_3}(s)}{\dot{m}_{urea}(s)} = \frac{1}{\tau s + 1}(1 - e^{-x/L})\eta_{NH_3} \tag{2.4}$$

$$\frac{\dot{m}_{HNCO}(s)}{\dot{m}_{urea}(s)} = \frac{1}{\tau s + 1}(1 - e^{-x/L})\eta_{HNCO} \tag{2.5}$$

where $\dot{m}_{urea}$ is the rate of urea injection in g/sec, $\dot{m}_{NH_3}$ and $\dot{m}_{HNCO}$ are the rate of formation of NH_3 and HNCO in g/sec, η_{NH_3} and η_{HNCO} are the efficiency of urea to NH_3 and urea to HNCO conversion, respectively.

Temperature of the catalyst brick is not measured directly in many studies. Instead, it can be estimated by using a single temperature sensor upstream of the SCR catalyst brick and a simple thermal model like the one in [19]. Engine-out NOx can be

measured without worrying about cross-sensitivity because the NOx sensor is usually placed upstream of the DEF injector.

For strategies that require the NH_3 storage fraction, it can be estimated by using dynamic model-based observers like the one developed in [10]. Simpler, linearized model-based observers, like the one in [20], are also used commonly to decrease computational complexity when implemented on a microcontroller.

2.3 Mathematical Models

Accurate mathematical models of the SCR system involve the use of Partial Differential Equations (PDEs) to capture mass, momentum, heat transfer and chemical kinetics. Such high-fidelity models would require enormous amounts of computational power and/or time to run. Nevertheless, they may be used for validation of simpler models and for testing controllers.

For real-time control applications, simpler models are required. Reference [11] models the system using a static lookup table that is based on engine speed and load combined with a variable time delay combined with a variable lead-lag coefficient filter. Linearized models are also used, as in [12], by linearizing a higher-order model at a certain operating condition. The drawback with this approach is that the model becomes increasingly inaccurate as the real system moves away from the operating point.

A better balance between computational complexity and model performance can be struck by using a lumped zero-dimensional model with the Continuously Stirred Tank Reactor (CSTR) assumption and is commonly used in the literature. The model can either be three-state or four-state depending on whether NO and NO_2 are lumped together as NOx or treated as separate species, respectively. References [21], [25], [26] and [27] use the three-state model, while [20], [28] and [29] use the four-state model.

2.4 Control Algorithms

Open-loop strategies were used initially to reduce tailpipe NOx. Reference [13] used an open-loop strategy. The ammonia-to-NOx ratio at the inlet was maintained close to one in order to maintain the stoichiometric ratio between NH_3 and NOx. The increasingly stringent regulations necessitated closed-loop control strategies and advanced control algorithms.

Closed-loop control strategies often use a simple feedforward term to target NOx reduction combined with NOx feedback. Reference [11] uses a model-based closed-loop control algorithm. A simple model-based feedforward strategy was combined with gain-scheduled NOx-feedback PI controller. The proportional and integral constants were changed based on the difference between tailpipe NOx and the NOx reference. Reference [19] combined a primary feedforward controller with a simplified storage fraction observer and a NOx-feedback PI controller. Since the NOx sensor is cross-sensitive to NH_3, an excitation filter is used in an attempt to gauge the true tailipipe NOx value. NOx reduction of 82% was achieved while keeping the average NH_3 slip below 10 ppm.

In [12], a closed-loop controller with self tuning strategy was presented. A parameter update law using least-squares with an exponential forgetting technique was employed. A NOx reduction of 84% was seen, while keeping the peak slip below 55 ppm and the mean slip below 7 ppm on a Cummins heavy-duty engine. This self-tuning feature can be seen as an extension of the gain-scheduled feedback term presented in [11].

Reference [20] used a full-state feedback nonlinear control law and appended a correction term that depends on the sign of error, combined with a tunable control variable. A linearized model-based observer is used to estmate the NH_3 storage term. The paper demonstrates the superiority of using a four-state model in the controller, in which NO and NO_2 are treated as separate species rather than combining them together and assuming all the incoming NOx is NO.

Several other advanced control strategies have been proposed. A sliding mode control framework is used in [21]. Reference [22] uses an adaptive Model Predictive Control (MPC) strategy with as many as 24 different linearized plant models in an attempt to reduce computational effort. This controller showed reduced variability in performance under changing conditions. Reference [28] uses a two-cell catalyst in which a high NH_3 storage is targeted for the first cell to achieve maximum NOx reduction, while a lower NH_3 storage is targeted for the second cell to help minimize NH_3 slip.

3. EXPERIMENTAL SETUP

To evaluate the performance of the various control algorithms in simulation and to run the SCR plant model, various data sets consisting of signals such as the engine-out NOx, catalyst bed temperature and exhaust flow rate for multiple drivecycles that represent real-world driving conditions are required. In this chapter, the experimental setup, along with the various sensing equipment and data acquisition systems that were used by our research group, are discussed.

3.1 Experimental Platform

The experiments to obtain the data sets mentioned above were performed on the 2013 Chevrolet Malibu that was used for the EcoCAR2 competition. It was retrofitted with a 1.7 L turbocharged diesel engine with Exhaust Gas Recirculation (EGR) capability and is shown in Figure 3.1. The car was hybridized using a Parallel-Through-The-Road (PTTR) architecture. The diesel engine powers the front wheels with a peak power of 96 kW at 2500 RPM. For the current project, the data sets were obtained by running the car in the engine-only mode.

3.1.1 Urea-SCR System

The car is equipped with a DOC-DPF-SCR aftertreatment system shown in Figure 3.2, which is installed on the underfloor of the car. The SCR catalyst is Vanadium-based and contains 1-3% V_2O_5 and about 10% WO_3 on the TiO_2 support [30]. The volume of the catalyst is 0.00371 m^3. The cell density and catalyst age are unknown and are identified as parameters.

A Bosch DeNOxtronic 3.1 DEF dosing unit is used to dose DEF into the exhaust gas stream. This unit consists of an injector that is solenoid-actuated and is shown in

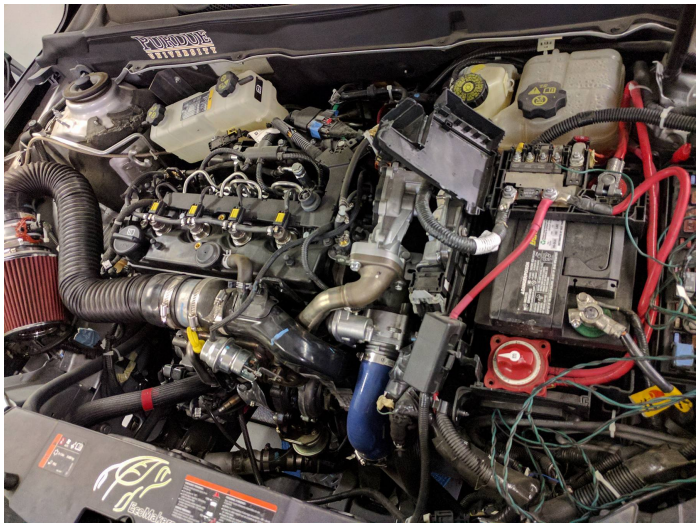

Figure 3.1. The EcoCAR2 engine bay

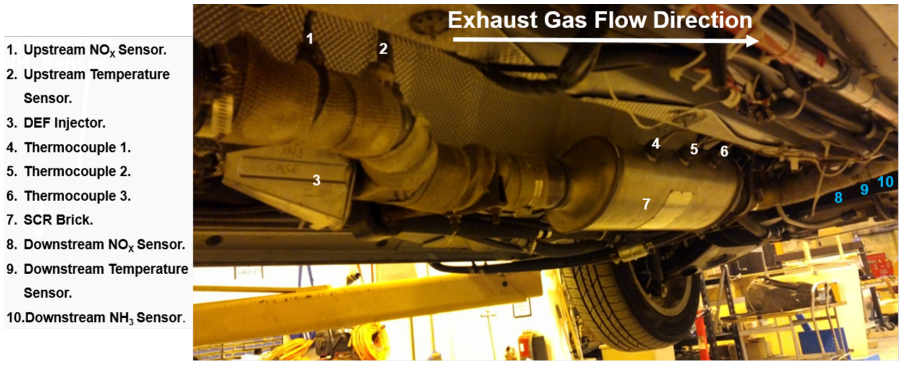

Figure 3.2. Urea-SCR system mounted on Purdue EcoCAR2 (Parts numbered in blue are not visible but are mounted in the shown order).

Figure 3.3. The injector is driven by a 12 V saturated switch driver at 4 Hz frequency with a 6 A Low Side Output (LSO) driver providing the driving signal from the microcontroller. The relationship between the injector's duty cycle and mass flow rate of the DEF solution was calibrated and was found to be:

$$m_{DEF} = 0.001(8.7274(DutyCycle) + 5.1673). \tag{3.1}$$

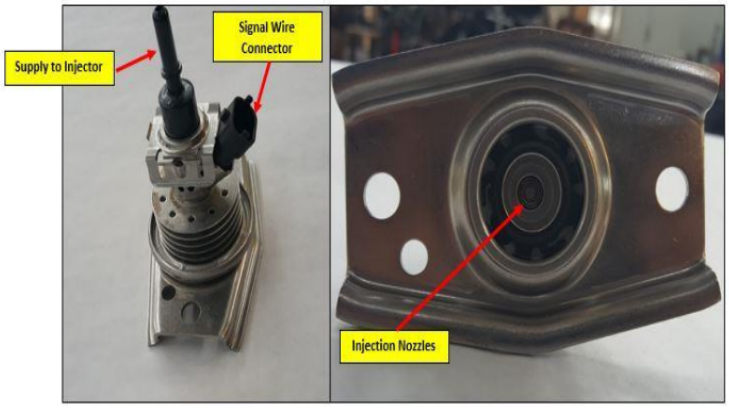

Figure 3.3. Bosch DeNoxtronic injector (taken from [8]).

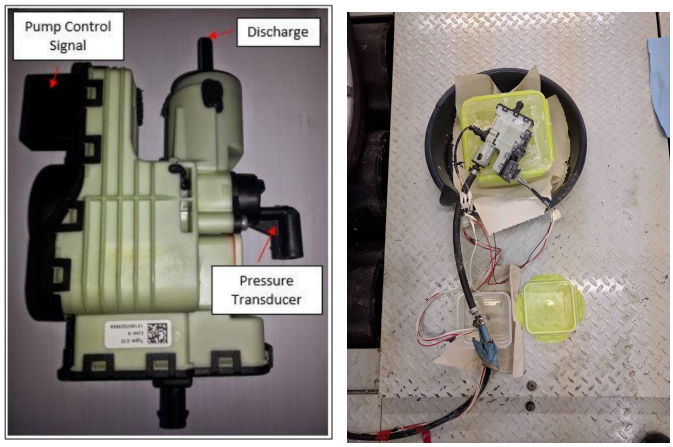

(a) (b)

Figure 3.4. Urea dosing pump, (a) with labeled components (taken from [8]) (b) mounted on the urea storage tank.

Figure 3.4(b) shows the assembly of the Urea SCR system with the DEF reservoir, supply unit, and supply lines. The Bosch DeNoxtronic 3.1 DEF supply unit consists of (i) a DC-motor-driven reciprocating diaphragm pump, and (ii) an inbuilt pressure transducer as shown in Figure 3.4(a) [8]. The supply unit requires a 12 V power supply. This is provided by the Woodward SECM112 microcontroller. The DC motor inside the supply unit is controlled by varying the duty cycle of a 980 Hz PWM (Pulse Width Modulated) pump control signal. A constant DEF delivery pressure of 5 bar

(72 psi) is maintained by using a feedback control strategy. The delivery pressure is measured by the pressure transducer that transmits a voltage in the range of 0.5 V to 4.5 V and is received by an analog pin of the SECM112 controller as a 10-bit ADC (analog to digital count) value [8].

3.2 Measurements

3.2.1 NH_3 Concentration

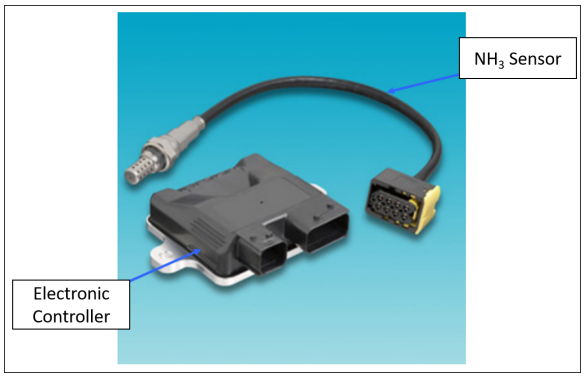

Figure 3.5. NH_3 sensor from Delphi (image from [31]).

A ceramic metal-oxide sensor from Delphi was used to measure the concentration of NH_3 in the exhaust gas, downstream of the SCR catalyst in parts per million (ppm). Communication between the NH_3 sensor and the microcontroller occurs via the CAN bus by sending a dewpoint byte to the sensor to either enable or disable it. The sensor transmits 8 bytes of data upon activation. The specifications of the NH_3 sensor are tabulated in Table 3.1. The various output signals received by the microcontroller from the NH_3 sensor are listed in Table 3.2. No cross-sensitivity is observed in the NH_3 sensor to the other species present in the exhaust stream, making this sensor very reliable. The sensor components are shown in Figure 3.5.

Table 3.1. NH_3 sensor specifications (taken from [31]).

Specifications	**Values**
NH_3 concentration measurement range	0 to 6500 ppm
NH_3 concentration measurement resolution	0.1 ppm
Maximum sampling frequency	1 Hz
Operating temperature range	200 to 500 °C
Nominal voltage range	13.5 V to 32 V
Maximum operating voltage	36 V
Minimum operating voltage	11 V
Data transfer rate	250 kbps or 500 kbps

Table 3.2. NH_3 sensor output signals (taken from [8]).

Signal Name	**Meaning**
$[NH_3]$	Concentration of NH_3 in ppm
Sensor Enable	Indicates if the sensor has been enabled
NH_3 Validity	Indicates if the NH_3 reading is valid
Sensor at Temperature	Indicates if the ceramic has reached its operating temperature
FMIs	Indicate if there are any short or open circuits

3.2.2 NOx Concentration

Gen 2.1 Ceramic metal-oxide sensors from Continental are used for onboard NOx measurements. The sensors are placed at two locations: upstream and downstream of the SCR catalyst. The various components of the sensor are shown in Figure 3.6(a). The specifications of the sensors are listed in Table 3.3. The various output signals that the NOx sensor provides are listed in Table 3.4. The NOx sensor also measures

the O_2 concentration as a percentage of the exhaust. Both these measurements are fed to the microcontroller via the CAN bus as binary numbers. These binary values are then converted to the appropriate units using calibration equations specified by the sensor manufacturer.

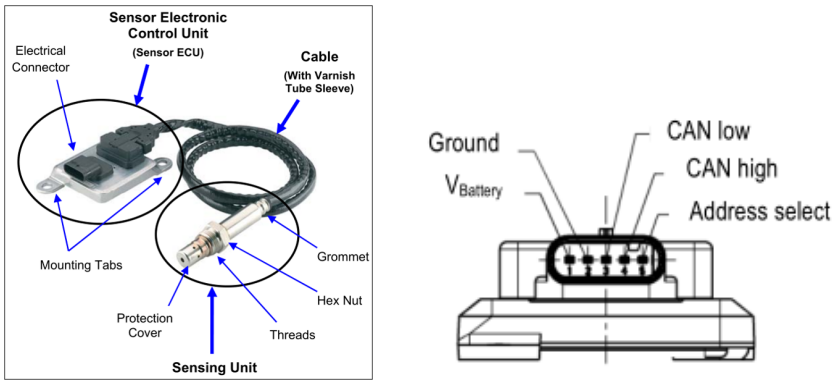

(a) (b)

Figure 3.6. Continental Gen 2.1 Smart NOx sensor with (a) labeled components and (b) its pin configuration (taken from [32]).

The sensor is turned on only when the exhaust gas is at a temperature at or above 210 °C. The reason behind this is to prevent any damage to the sensor. The ceramic in the sensor is heated up during its interaction with exhaust gases. Any contact between the heated ceramic and liquid droplets would damage the sensor permanently. At 210 °C the probability of liquid water droplets being present in the exhaust stream is very low.

The primary drawback of the Continental Gen 2.1 Smart NOx sensor is that it is cross sensitive to NH_3. The NOx reading is therefore altered in the presence of NH_3. Further, the cross-sensitivity changes with temperature. It is important to note that the upstream NOx sensor is not affected because the NH_3 concentration is zero at its location. The NOx sensors are not required for the control algorithms developed in Chapter 5 but are required to perform system identification.

Table 3.3. NOx sensor specifications (taken from [8]).

Specifications	**Values**
NOx concentration measurement range	0 to 3000 ppm
NOx measurement accuracy (for 0 to 1500 ppm)	+/-20 ppm (for 0 to 100 ppm) +/-20 % (for 100 to 1500 ppm)
O_2 concentration measurement range	0 to 21 %
NOx response time	1650 ms
O_2 response time	1300 ms
Maximum sampling frequency	1 Hz
Operating temperature range	200 to 800 °C
Supply current	1.5 A
Supply voltage	10.8 V to 16 V
Data transfer rate	250 kBaud

Table 3.4. NOx sensor output signals (from [8], [32]).

Signal Name	**Meaning**
[NOx]	Concentration of NOx in ppm
[O_2]	Concentration of O_2 in %
Power in Range	Indicates if the voltage supply is within acceptable range
Sensor at Temp	Indicates if the ceramic has reached its operating temperature
NOx Stable	Indicates if the [NOx] signal is valid
O_2 Stable	Indicates if the [O_2] signal is valid
Heater Control	Indicates the heating up condition of the ceramic
Heater, NOx and O_2 FMI (Failure Mode Indicator)	Indicates if there's an error due to short or open circuit

3.2.3 Temperature Measurement

Catalyst bed temperatures were measured using K-type thermocouples, and exhaust gas temperatures were measured using Resistance Temperature Detectors (RTDs).

3.2.3.1 Catalyst Bed Temperature

Three K-type thermocouples are used for catalyst bed temperature measurement. One thermocouple is placed in the middle of the SCR catalyst and the other two thermocouples are placed equidistantly along the direction of flow of the exhaust gas from the one in the middle. These thermocouples sample temperatures at a frequency of 1 Hz, which is much faster than the temperature dynamics of the system. These temperature signals after linearization and amplification by an amplifier circuit (Figure 3.7(b)) are fed to the microcontroller as 10-bit ADC values. The calibration equations (from [8]) are:

$$T_{T1} = 0.962(ADC1) - 245.86 \tag{3.2}$$

$$T_{T2} = 0.9722(ADC2) - 248.12 \tag{3.3}$$

$$T_{T3} = 0.9655(ADC3) - 247.98 \tag{3.4}$$

These calibration curves are shown in Figure 3.8. where T_{Ti} is the temperature measured by the thermocouple T_i in °C, and ADC_i is the corresponding ADC value. The arithmetic mean of the three sensor measurements is used for the single-cell CSTR model in this project.

3.2.3.2 Exhaust Gas Temperature

The exhaust gas temperature is measured upstream and downstream of the SCR catalyst using one Resistance Temperature Detector (RTD) mounted at each of these

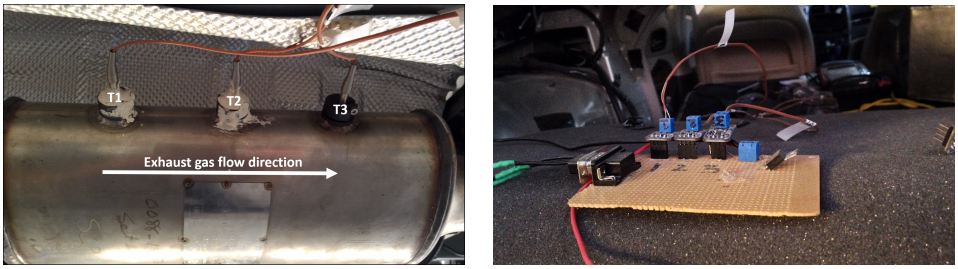

(a) (b)

Figure 3.7. Catalyst bed temperature measurement apparatus: (a) K-type thermocouples labeled as T1, T2 and T3, (b) Amplifier circuit.

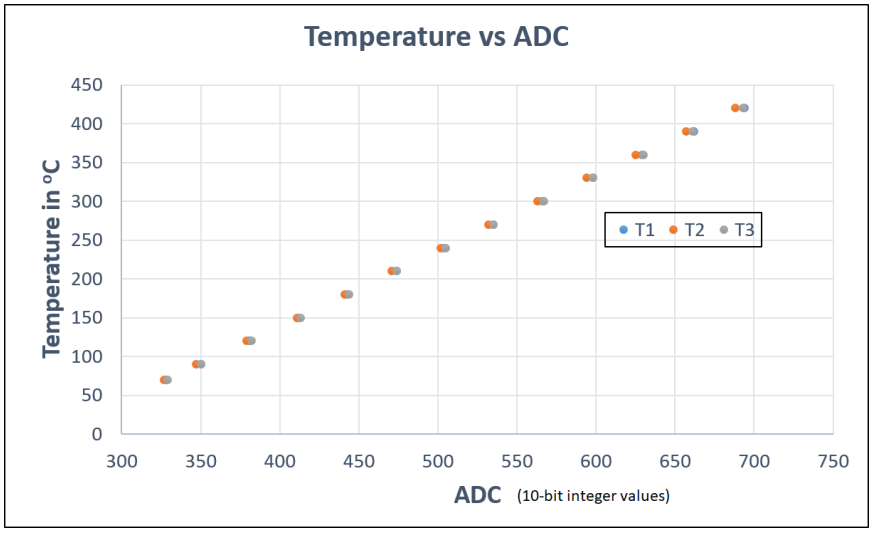

Figure 3.8. Thermocouple calibration curves.

locations. These RTDs sample temperature at a frequency of 1 Hz. The temperature signals are fed to the microcontroller as 10-bit ADC values. The calibration equations for the RTDs are:

$$T_{RTD_{upstream}} = 2.5692(ADC_{upstream}) - 482.16 \tag{3.5}$$

$$T_{RTD_{downstream}} = 2.5728(ADC_{downstream}) - 466.54 \tag{3.6}$$

where $T_{RTD_{upstream}}$ and $T_{RTD_{downstream}}$ are the temperatures measured by the RTD upstream and downstream of the catalyst, in °C, respectively, and ADC is the corresponding ADC value received by the micro-controller. The two calibration curves are shown in Figure 3.9.

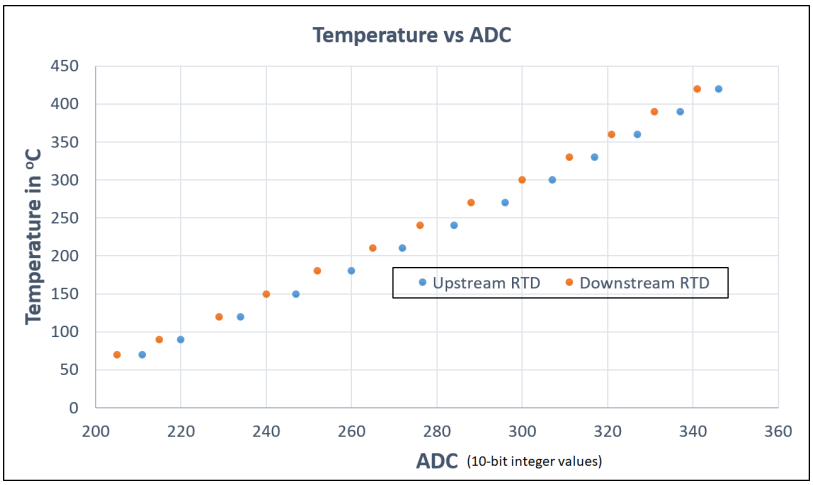

Figure 3.9. RTD calibration curves.

3.2.3.3 Exhaust Gas Mass Flow Rate

The exhaust gas mass flow rate is not measured directly. Instead, the principle of conservation of mass is used. The mass flow rate of the exhaust gas is given by:

$$\dot{m}_{exhaust} = \dot{m}_{air} + \dot{m}_{fuel} \tag{3.7}$$

where $\dot{m}_{exhaust}$ is the mass flow rate of exhaust gas, $\dot{m}_{air}$ is the mass flow rate of air going into the engine, and $\dot{m}_{fuel}$ is the mass flow rate of fuel going into the engine. The $\dot{m}_{air}$ and $\dot{m}_{fuel}$ signal values are requested from the Engine Control Module at a frequency of 10 Hz.

The volumetric flow rate of the exhaust gas is an essential quantity as it is necessary for running the SCR plant model in simulation and for the controller. It is

calculated from the exhaust gas mass flow rate using Equation 3.8, which is obtained from the ideal gas law.

$$\dot{V}_{exhaust} = \frac{\dot{m}_{exhaust} RT}{M_{exhaust} P_{ambient}} \tag{3.8}$$

where $\dot{V}_{exhaust}$ is the volumetric flow rate in m^3/s. $\dot{m}_{exhaust}$ is the exhaust gas mass flow rate in kg/s, $M_{exhaust}$ is the molar mass of the exhaust gas in kg/mol, T is the temperature of the exhaust gas in K, R is the universal gas constant in J/mol-K and $P_{ambient}$ is the ambient atmospheric pressure in Pa.

3.3 Data Acquisition

3.3.1 Urea-SCR Microcontroller

A Woodward SECM112 microcontroller is used for the control of the Urea-SCR system for communication with the various sensors and actuators. The microcontroller consists of two different microprocessors. The primary microprocessor is a 32-bit Freescale MPC564xA. The secondary microprocessor is a 16-bit MC9S12G. The microcontroller is powered using a 12 V supply from the vehicle's low voltage circuit. Appropriate voltage protection for the microcontroller, the various actuators, and thermocouple amplifiers is required to prevent damage to the system. The specifications of the microcontroller are listed in Table 3.5. The microcontroller is shown in Figure 3.10.

Figure 3.10. Woodward SECM112 Micro-controller (taken from [8]).

Table 3.5. Woodward SECM112 specifications [8].

Specifications	Values
Number of analog channels	33
Number of CAN channels	3
Number of low side output channels	16
Number of transducer outputs	3
Input voltage	10 to 32 V
Rated power capability	0.8 kW

3.3.2 CAN Bus Communication

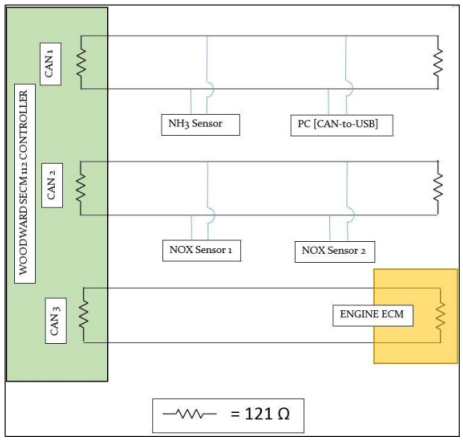

Figure 3.11. CAN bus wiring diagram (taken from [8]).

Communication between the Woodward SECM112 microcontroller and the NOx and NH_3 sensors, and the ECM is established using the CAN channels on the microcontroller. The data transfer rates of the various CAN channels are shown in Table 3.6. J1939 CAN bus cables and external resistances of 121 Ω at the ends of CAN 1 and CAN2 are used for the required wiring. The CAN bus wiring diagram is shown in Figure 3.11.

Table 3.6. CAN Bus Transfer Rates [8].

Channel	Data Transfer Rate
CAN1	500 kBaud
CAN2	250 kBaud
CAN3	500 kBaud

3.4 Testing Equipment

3.4.1 Chassis Dynamometer

A Mustang AWD500 Series four-wheeled chassis dynamometer (shown in Figure 3.12) was used for the purpose of testing and conducting experiments on the EcoCAR2 by emulating real-world driving conditions and various standard drivecycles in a controlled laboratory environment. A schematic diagram of the chassis dynamometer is shown in Figure 3.13.

Figure 3.12. Mustang AWD500 Series Chassis Dynamometer.

The major components of the dynamometer are listed below.

1. Chassis: This structure encloses and supports the dynamometer components like the friction rollers, the PAUs (Power Absorption Units), and the mounting harnesses.

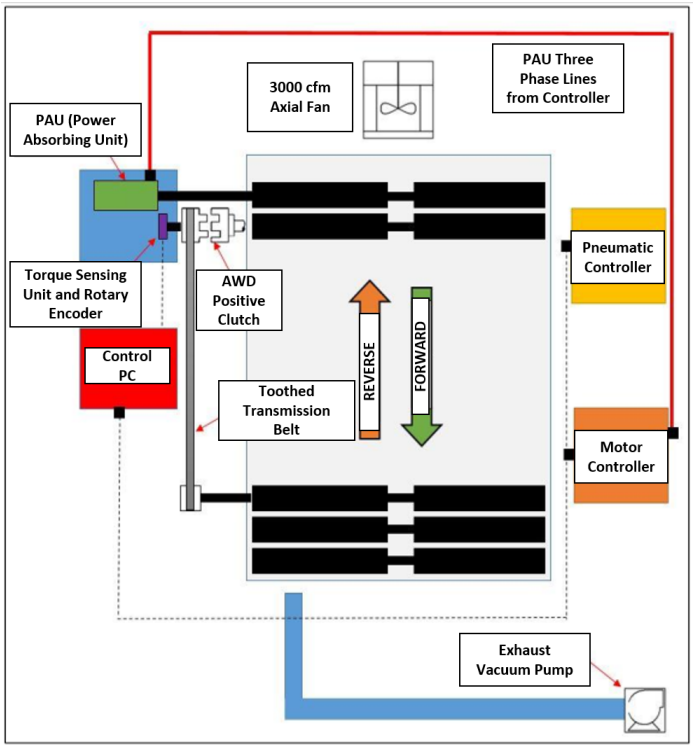

Figure 3.13. Mustang Dynamometer's schematic (taken from [8]).

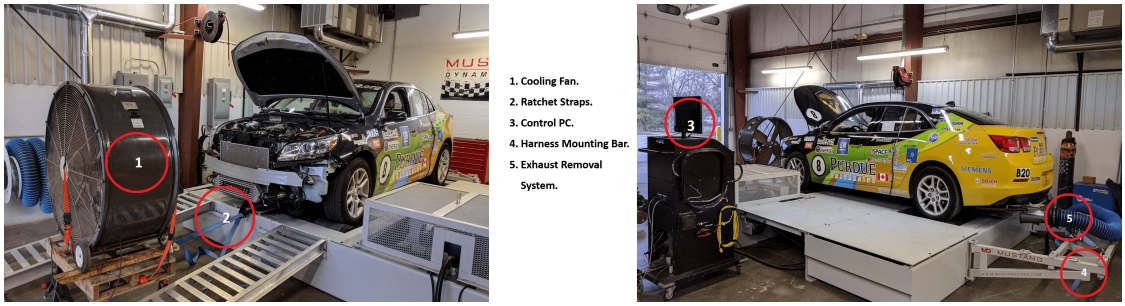

(a) (b)

Figure 3.14. Photographs of EcoCAR2 on the Mustang dynamometer taken from the car's (a) front left, and (b) back left.

2. Friction rollers: The friction rollers are double-contact-type rollers and are the point of contact between the vehicle and the dynamometer. They are shown in Figure 3.13. There are three rollers in the front and two in the back to accommodate vehicles of different wheelbases.

3. Ratchet straps: They are used to secure the vehicle to the dynamometer chassis and prevent lateral motion during testing. These are attached to the ground on one end and to the harness mounting bars on the other, as shown in Figure 3.14(a).

4. PAU controller: The Mustang dynamometer has two PAUs, as shown in Figure 3.15. The PAU controller runs either the AC motor PAU or eddy current PAU or both to apply the desired load/speed/power on the vehicle based on the torque measurements from load cell 1 or 2.

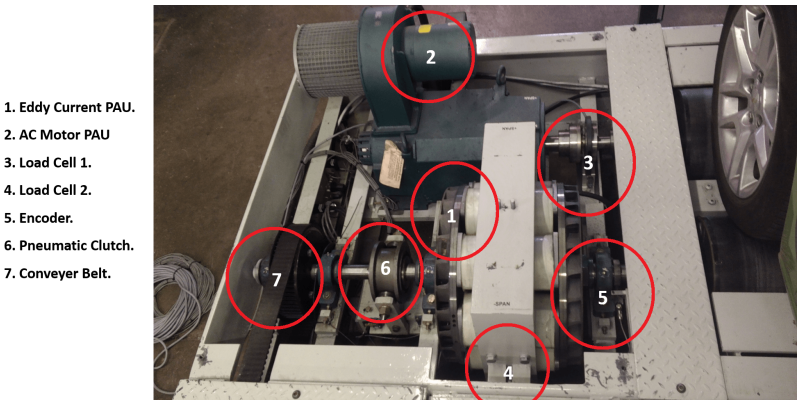

Figure 3.15. PAU bay of the Mustang dynamometer.

5. Pneumatic controller: The pneumatic controller actuates the front and rear lifts under the friction rollers and the clutch located in the PAU bay. The lifts are responsible for locking and unlocking the respective rollers as required. The clutch is needed to couple or decouple the rollers to operate the dynamometer in AWD (All Wheel Drive)/2WD (Two Wheel Drive) mode.

6. Control PC: PowerDyne software, which is installed on the control PC, allows us to interface with the dynamometer for performing various operations such as load cell calibration, controlling the lift or the clutch, and performing a variety of tests. It also stores test data files and the calibration files.

7. Exhaust suction: This provides a direct pathway between the tailpipe of the car and the outside environment outside the dynamometer test facility to prevent suffocation inside the facility. A vacuum pump is employed to enable suction of the exhaust gases.

8. Cooling fan: The car is static while being tested on the dynamometer, and its engine can overheat due to the absence of forced convection from fast-flowing air. The 0.5 HP constant-speed cooling fan allows for cooling of the engine radiator through forced convection.

3.5 Experimental Data

Data was gathered from the EcoCAR2 for several steady-state and transient drive-cycles with several different objectives listed in references [8, 10]. For the current project, data sets containing the SCR operating conditions (catalyst bed temperature, engine-out NOx, and flow rate of exhaust gas) are required to evaluate the performance of the controller over multiple different drivecycles. An artificial set of data developed in reference [33] was also used so as to contain a mix of steady-state and transient conditions. Figures 3.16-3.18 contain plots of the engine-out NOx, flow rate of exhaust gases and the catalyst bed temperature data obtained by running the car on the UDDS, Artifical and HWFET drivecycles. These signals are needed since they are passed as inputs to validate the SCR model described in Chapter 4 and to test the control algorithms developed in Chapter 5.

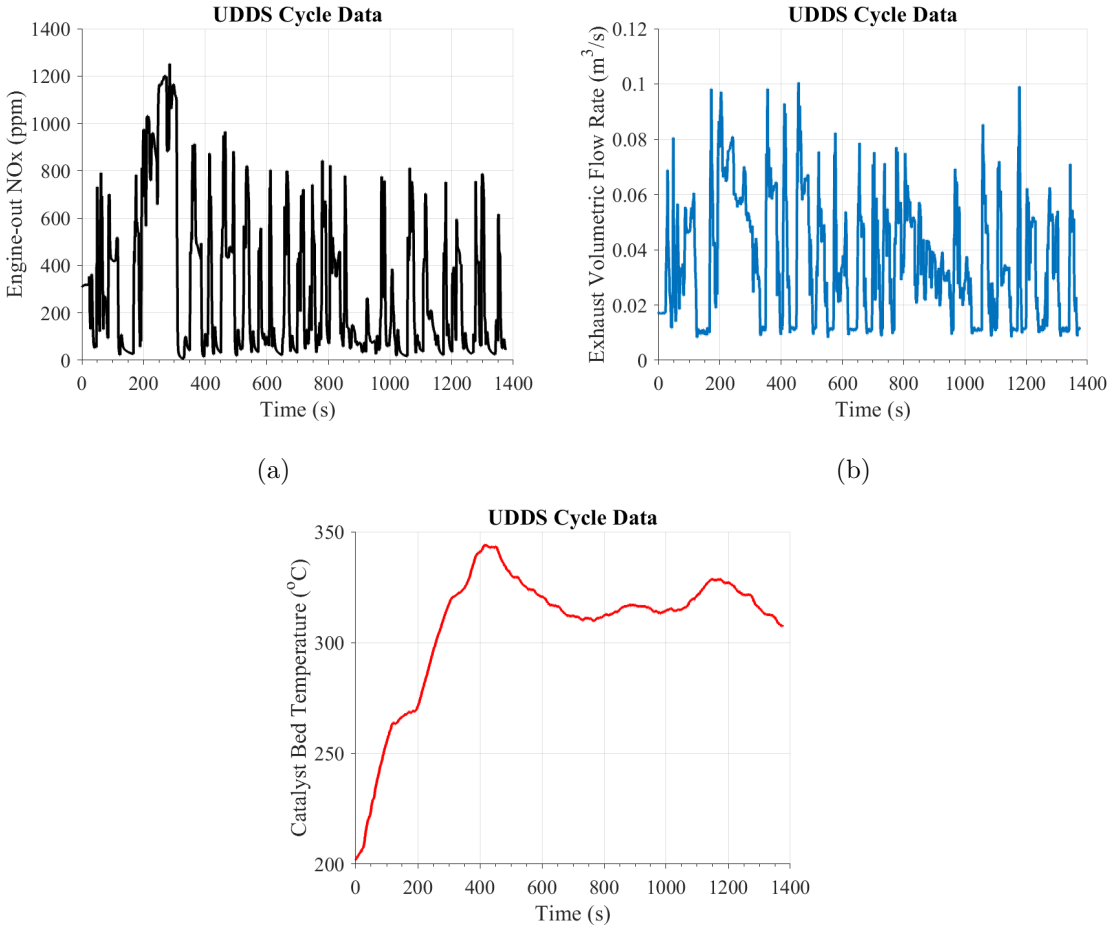

Figure 3.16. Experimentally-obtained SCR inlet conditions. The plots of (a) Engine-out NOx (b) Volumetric flow rate of exhaust gases, and (c) Temperature of the SCR catalyst bed obtained by running the UDDS drivecycle on the car

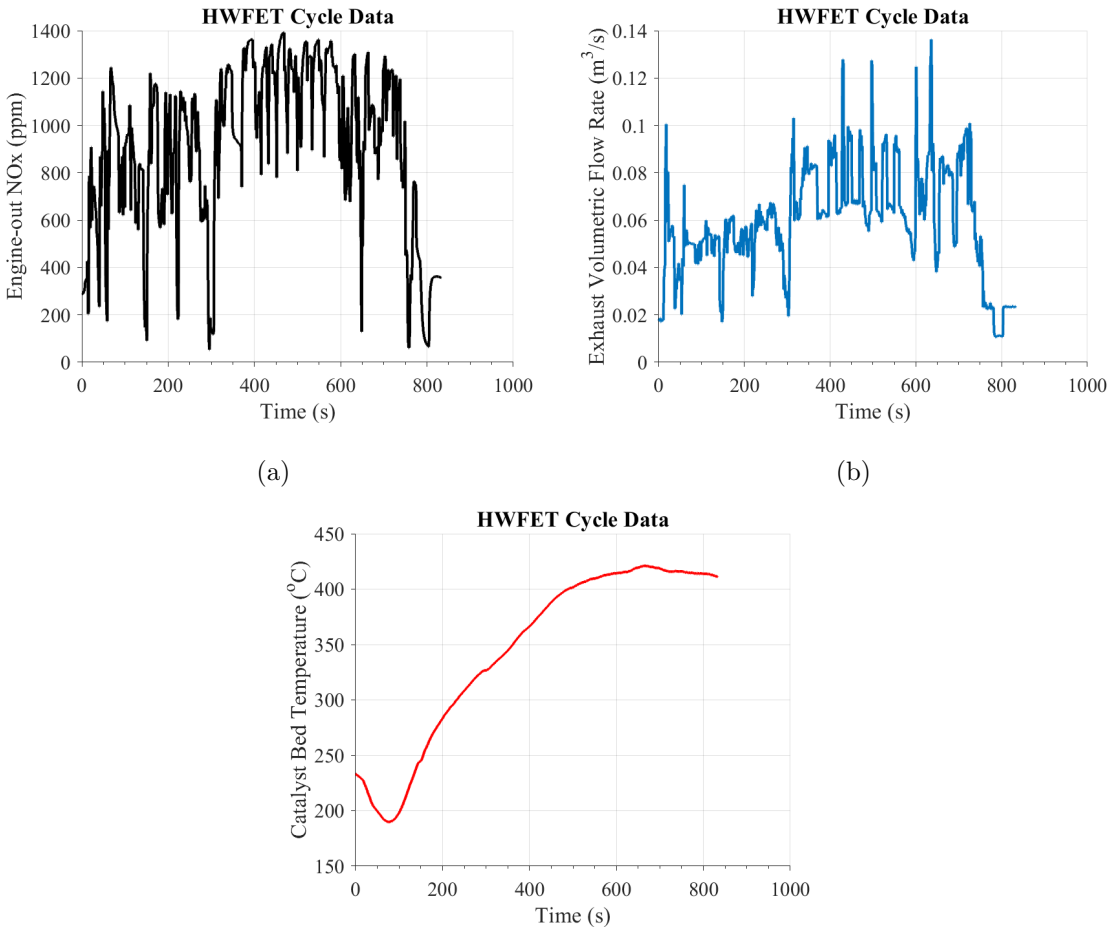

Figure 3.17. Experimentally-obtained SCR inlet conditions. The plots of (a) Engine-out NOx (b) Volumetric flow rate of exhaust gases, and (c) Temperature of the SCR catalyst bed obtained by running the HWFET drivecycle on the car

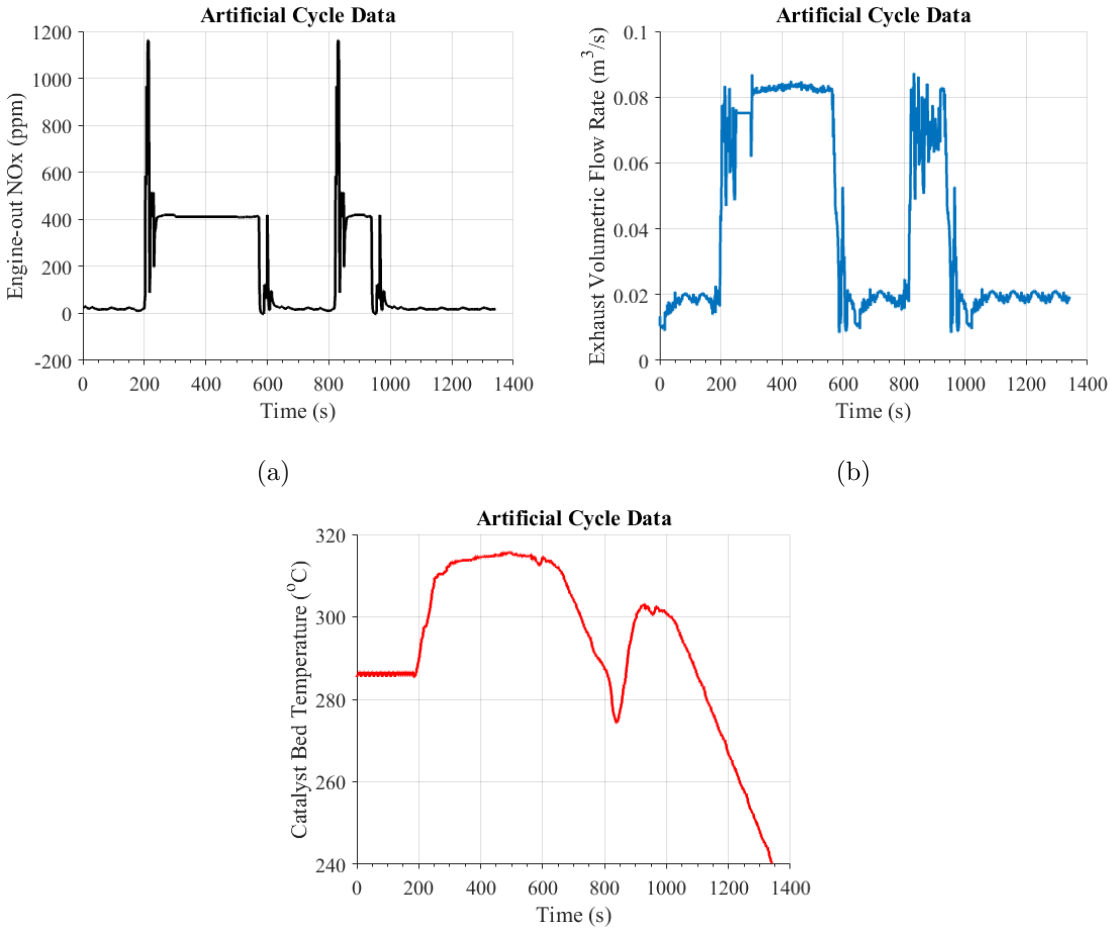

Figure 3.18. Experimentally-obtained SCR inlet conditions. The plots of (a) Engine-out NOx (b) Volumetric flow rate of exhaust gases, and (c) Temperature of the SCR catalyst bed for the Artificial drive-cycle.

4. MODELING AND SIMULATION

The design of good control strategies for the urea dosing controller requires the algorithm designer to test several different control strategies and to try improving them in every design iteration. Directly testing all of these strategies on an experimental setup would cost a lot of time and money. Further, it could result in the aging of the Urea-SCR system due to extended periods of exposure to high temperatures. This motivates the need to test the control strategies in simulation before implementing them on the SCR control unit in the vehicle. The SCR model used for the simulations must capture the dynamics of the system and must represent the actual SCR system closely.

4.1 The CSTR Model

Modeling the Urea-SCR system with high fidelity would require the use of partial differential equations to capture the physics of heat transfer, mass transfer, and momentum transfer. Such models, though precise, are computationally very expensive and make the design process cumbersome as they could take a very long time to run even on a powerful computer. They are also unsuitable for real-time control applications. Several sources in the literature ([28, 30]) have modeled the Urea-SCR system as a Continuous Stirred Tank Reactor (CSTR). The same approach is used to model the SCR system in the current study. A schematic for the CSTR model is shown in Figure 4.1. The CSTR model is a lumped-parameter zero-dimensional model that assumes homogenous distribution of reacting elements in the catalyst. This perfect mixing assumption means that the composition of various species at the output is identical to their composition inside the Urea-SCR system.

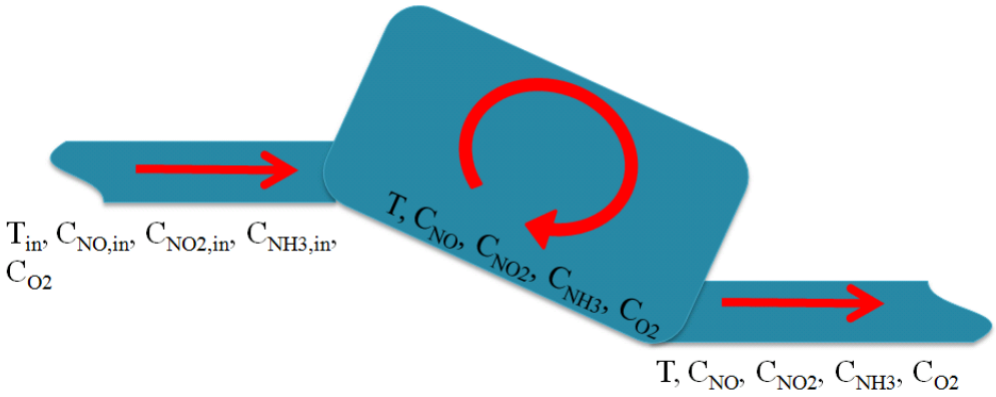

Figure 4.1. Schematic Diagram of the CSTR model from [28]

4.1.1 Reactions

The injector in the Urea-SCR system injects Diesel Exhaust Fluid (DEF), which is a 32.5% aqueous solution of urea. A large number of reactions occur in the Urea-SCR system. Many of these reactions produce species in minor amounts that are not of interest in this study and are therefore not considered. The main reactions considered in the control-oriented model are listed in Equations 4.1 to 4.8.

The injected urea undergoes thermolysis and hydrolysis. One molecule of urea can result in up to two molecules of ammonia in the gaseous phase, depending on the physical conditions such as temperature. For the rest of the reactions, the Eley-Rideal mechanism, which is widely accepted for reactions on surfaces, is used to capture the Urea-SCR chemical dynamics. The Eley-Rideal mechanism pertaining to reactions between two different species suggests that only one of these species is adsorbed onto the catalyst and the other reacts with it directly from the gas phase. In the Urea-SCR system, a fraction of the gas phase NH_3 is adsorbed onto the catalyst surface while the remaining gas-phase ammonia and undissociated urea exit the system unused. A fraction of the NH_3 adsorbed reacts with gaseous phase NOx or undergoes oxidation

while the rest is desorbed. The unadsorbed NH_3 combined with the desorbed NH_3 can be measured at the tailpipe as NH_3 slip.

1. Urea to NH_3 conversion

   Thermolysis:

$$(NH_2)_2CO \longrightarrow HNCO + NH_3 \tag{4.1}$$

   Hydrolysis:

$$HNCO + H_2O \longrightarrow NH_3 + CO_2 \tag{4.2}$$

2. NH_3 Adsorption

$$NH_3 + \theta_{\text{free}} \longrightarrow NH_3(\text{ads}) \tag{4.3}$$

   where θ_{free} is the number of moles of catalyst sites available for NH_3 adsorption.

3. NH_3 Desorption

$$NH_3(\text{ads}) \longrightarrow NH_3 + \theta_{\text{free}} \tag{4.4}$$

   where θ_{free} is the number of moles of catalyst sites available for NH_3 adsorption.

4. NOx Reduction

   Standard SCR reaction:

$$4\,NH_3(\text{ads}) + 4\,NO + O_2 \longrightarrow 4\,N_2 + 6\,H_2O \tag{4.5}$$

   Fast SCR reaction:

$$4\,NH_3(\text{ads}) + 2\,NO + 2\,NO_2 \longrightarrow 4\,N_2 + 6\,H_2O \tag{4.6}$$

   Slow SCR reaction:

$$8\,NH_3(\text{ads}) + 6\,NO_2 \longrightarrow 7\,N_2 + 12\,H_2O \tag{4.7}$$

5. NH_3 Oxidation

$$4\,NH_3(ads) + 3\,O_2 \longrightarrow 2\,N_2 + 6\,H_2O \tag{4.8}$$

The Arrhenius equation is used to obtain reaction rates. It expresses reaction rates as a function of concentrations of the reacting species and temperature.

1. NH_3 adsorption: The rate of occupation of NH_3 adsorption sites on the SCR catalyst and the rate of consumption of NH_3 from the gaseous phase are equivalent and are given by

$$R_{ads} = A_{ads} e^{\frac{-E_{ads}}{RT}} C_{NH_3} C_{\theta_{free}} \tag{4.9}$$

2. NH_3 desorption: The rate at which the NH_3 molecules adsorbed on the SCR catalyst leave the surface and reenter the gaseous phase is given by

$$R_{des} = A_{des} e^{\frac{-E_{des}}{RT}} C_{NH_3(ads)} \tag{4.10}$$

3. Standard SCR reaction: The rate of reduction of NO and the rate of consumption of NH_3 for the standard SCR reaction are equivalent and are given by

$$R_{std} = A_{std} e^{\frac{-E_{std}}{RT}} C_{NH_3(ads)} C_{NO} \tag{4.11}$$

4. Fast SCR reaction: The rates of reduction of NO and NO_2 and the rate of consumption of adsorbed NH_3 are equivalent and are given by

$$R_{fast} = A_{fast} e^{\frac{-E_{fast}}{RT}} C_{NH_3(ads)} C_{NO} C_{NO_2} \tag{4.12}$$

5. Slow SCR reaction: The rate of reduction of NO_2 and rate of consumption of adsorbed NH_3 and are given by

$$R_{slow} = A_{slow} e^{\frac{-E_{slow}}{RT}} C_{NH_3(ads)} C_{NO_2} \tag{4.13}$$

6. NH_3 oxidation rate: The rate of oxidation of adsorbed NH_3 is given by

$$R_{oxi} = A_{oxi} e^{\frac{-E_{oxi}}{RT}} C_{NH_3(ads)}. \tag{4.14}$$

In the reaction rate equations (Equations 4.9 to 4.14) described above, R_i is the rate of the chemical reaction (with SI units of mol/s), E_i is the activation energy expressed in Joules, A_i is the pre-exponential factor (also known as the rate constant), T is the temperature of the catalyst bed in Kelvin, R is the universal gas constant (8.314 J / (mol·K)) and C_j is the concentration of species j expressed in moles/m^3.

The rate of the slow SCR reaction (Equation 4.13) is very slow in comparison to the other reactions listed above and can be neglected.

4.1.2 System Dynamic Equations

The system dynamics are modeled using the law of conservation of mass and the Arrhenius rate equations from the previous section. These laws for modeling the system dynamics are more conveniently applied when the concentrations of the various reacting species are in mol/m^3. The NOx and NH_3 sensors present onboard the vehicle, however, measure the concentrations of these species in parts per million (ppm). Thus, the species' concentrations will need to be converted to mol/m^3.

The number of moles of ammonia adsorbed onto the catalyst ($C_{NH_{3(ads)}}$) and the number of moles of available catalyst sites ($C_{\theta_{free}}$) are given by:

$$\begin{bmatrix} C_{NH_3(ads)} \\ C_{\theta_{free}} \end{bmatrix} = \begin{bmatrix} x_3 K \\ (1 - x_3)K \end{bmatrix}. \tag{4.15}$$

where x_3 is the fraction of catalyst's NH_3 adsorption sites occupied by NH_3 molecules and K is the total number of catalyst's NH_3 adsorption sites available, in moles. K is a function of the catalyst bed temperature and changes as catalyst ages. It is modeled as:

$$K = S_1 e^{-S_2 T} \tag{4.16}$$

where S_1 and S_2 are functions of the catalyst's age.

The principle of conservation of mass to each of the species can now be applied to obtain the system dynamic equations.

Table 4.1. Symbols for quantity and concentration of reactants and products.

Species	**Quantity in moles**	**Concentration in moles/m^3**
NH_3	C_{NH_3}	x_1
NO	C_{NO}	$x_{2,NO}$
NO_2	C_{NO_2}	x_{2,NO_2}
NOx	C_{NOx}	x_2
NH_3 going into the catalyst	$C^{in}_{NH_3}$	u_1
NO going into the catalyst	C^{in}_{NO}	$u_{2,NO}$
NO_2 going into the catalyst	$C^{in}_{NO_2}$	u_{2,NO_2}
NOx going into the catalyst	C^{in}_{NOx}	u_2

$$\dot{C}_{NH_3} = \frac{C^{in}_{NH_3} - C_{NH_3}}{time} - R_{ads} + R_{des} \tag{4.17}$$

$$\dot{C}_{NOx} = \frac{C^{in}_{NOx} - C_{NOx}}{time} - R_{SCR} \tag{4.18}$$

and

$$\dot{C}_{NH_3(ads)} = -R_{SCR} + R_{ads} - R_{des} - R_{oxi} \tag{4.19}$$

Writing the total quantities of each of the species in terms of concentration using Table 4.1, we can write Equations 4.17 to 4.19 as:

$$\dot{x}_1 V = F(u_1 - x_1) - A_{ads} e^{\frac{-E_{ads}}{RT}} x_1 V(1 - x_3)K + A_{des} e^{\frac{-E_{des}}{RT}} x_3 K \tag{4.20}$$

$$\dot{x}_2 V = F(u_2 - x_2) - A_{SCR} e^{\frac{-E_{SCR}}{RT}} (x_2 V)(x_3 K) \tag{4.21}$$

$$\begin{aligned}\dot{x}_3 KV = &-A_{SCR} e^{\frac{-E_{std}}{RT}} (x_2 V)(x_3 K) + A_{ads} e^{\frac{-E_{ads}}{RT}} x_1 V(1-x_3)K \\ &- A_{des} e^{\frac{-E_{des}}{RT}} x_3 K - A_{oxi} e^{\frac{-E_{oxi}}{RT}} x_3 K\end{aligned} \tag{4.22}$$

where V is catalyst volume in m^3 and F is the exhaust gas volume flow rate in m^3/sec. Dividing Equations 4.20 and 4.21 by V and Equation 4.22 by KV we obtain:

$$\dot{x}_1 = \frac{F}{V}(u_1 - x_1) - A_{ads} e^{\frac{-E_{ads}}{RT}} x_1(1-x_3)K + \frac{A_{des}}{V} e^{\frac{-E_{des}}{RT}} x_3 K \tag{4.23}$$

$$\dot{x}_2 = \frac{F}{V}(u_2 - x_2) - A_{SCR} e^{\frac{-E_{SCR}}{RT}} (x_2)(x_3 K) \tag{4.24}$$

$$\begin{aligned}\dot{x}_3 = &-A_{SCR} e^{\frac{-E_{std}}{RT}} (x_2)(x_3) + A_{ads} e^{\frac{-E_{ads}}{RT}} x_1(1-x_3) \\ &- A_{des} e^{\frac{-E_{des}}{RT}} x_3 K - A_{oxi} e^{\frac{-E_{oxi}}{RT}} x_3 K\end{aligned} \tag{4.25}$$

Merging these three state equations into one matrix equation, we obtain

$$\begin{bmatrix} \dot{x}_1 \\ \dot{x}_2 \\ \dot{x}_3 \end{bmatrix} = \begin{bmatrix} \frac{F}{V}(u_1 - x_1) & 0 & -x_1(1-x_3)K & x_3 K & 0 \\ \frac{F}{V}(u_2 - x_2) & -(x_2)(x_3 K) & 0 & 0 & 0 \\ 0 & -(x_2)(x_3) & x_1(1-x_3) & -x_3 & -x_3 \end{bmatrix} \begin{bmatrix} 1 \\ A_{SCR} e^{\frac{-E_{SCR}}{RT}} \\ A_{ads} e^{\frac{-E_{ads}}{RT}} \\ \frac{A_{des}}{V} e^{\frac{-E_{des}}{RT}} \\ \frac{A_{oxi}}{V} e^{\frac{-E_{oxi}}{RT}} \end{bmatrix} \tag{4.26}$$

4.1.3 Urea to NH_3 conversion

The DEF injected into the exhaust gas stream by the urea injector is converted to NH_3 by the hydrolysis and thermolysis reactions. It is necessary to know the amount of NH_3 entering the SCR catalyst control volume in order to be able to employ model-based control strategies. Placing an NH_3 sensor upstream of the SCR catalyst is not viable because (i) any liquid urea/water droplets present in the exhaust gas stream would damage the sensor and (ii) it would increase total system cost. A model is therefore needed to estimate the rate at which gaseous NH_3 is entering the control volume.

The mass flow rate of DEF through the injector is related to the injector duty cycle. A calibration between the two quantities was performed and the calibration equation was found to be:

$$\dot{m}_{DEF} = 0.001(8.7274(DutyCycle) + 5.1673) \tag{4.27}$$

where $\dot{m}_{DEF}$ is in g/s. DEF is a 32.5% by weight aqueous solution of urea. Therefore, the rate of injection of urea in moles/s is :

$$\dot{n}_{urea} = \frac{0.325 \times \dot{m}_{DEF}}{60.06} \tag{4.28}$$

One mole of injected urea can result in a maximum of two moles of NH_3. The conversion of urea to NH_3 via hydrolysis and thermolysis upstream of the SCR inlet is modeled to have first-order dynamics. The concentration of NH_3 going into the SCR catalyst (u_1) is therefore given by:

$$\dot{u}_1 = \frac{1}{\tau}\left(-u_1 + \eta\frac{2 \times 0.325\dot{m}_{DEF}}{60.06F}\right) \tag{4.29}$$

where τ is the time constant and η is the efficiency of urea to NH_3 conversion.

4.2 Simulation

The state-space equations for the three-state model are implemented in a MATLAB/Simulink framework. The ode15s solver is used to simulate the differential equations. A schematic of the model is shown in Figure 4.2.

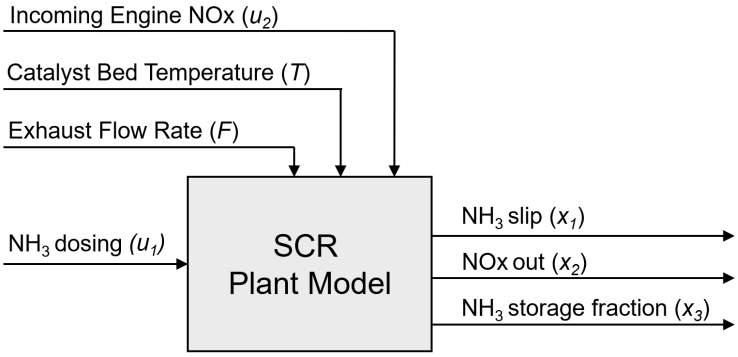

Figure 4.2. Schematic of the three-state Urea-SCR model.

4.2.1 Inputs

The model needs four input signals. The manipulated variable is the NH_3 entering the catalyst (u_1). The other three inputs are engine-out NOx (u_2), catalyst bed temperature (T), and the flow rate of exhaust gases (F) and are all measured disturbances.

1. Injected NH_3 (u_1): This is the concentration of NH_3 (in mol/m^3) present in the exhaust gas stream entering the SCR catalyst control volume. The conversion of urea to NH_3 is expressed in Equation 4.29.

2. Engine-out NOx (u_2): This is the concentration of NOx (in mol/m^3) present in the exhaust gas stream entering the SCR catalyst control volume. It consists primarily of NO and NO_2. The source of the NOx is combustion in the engine.

3. Catalyst bed temperature (T): This is the temperature of the SCR catalyst (in K). The mean temperature reading of the three thermocouples is used for this signal. The rates of reactions within the SCR catalyst are strong functions of temperature.

4. Exhaust volumetric flow rate (F): This is the flow rate of the exhaust gases (in m^3/s).

4.2.2 Outputs

The outputs of the system are obtained after evaluating the system dynamic equations using the input signals and system parameters. The outputs are stored as time-series vectors in the workspace for post-processing.

1. Tailipipe NH_3 Slip (x_1): This is the total concentration of NH_3 (in mol/m^3) from various sources (desorbed and unadsorbed NH_3) that appears at the tailpipe. Note that this is equivalent to the total gas-phase NH_3 concentration in the SCR at any given moment because of the CSTR approximation.

2. Tailpipe NOx (x_2): This is the concentration of the total NOx (in mol/m^3) at the tailpipe of the vehicle. This is equivalent to the total gas-phase NOx in the SCR control volume at any given moment due to the CSTR assumption.

3. Catalyst NH_3 Storage Fraction (x_3): This is the fraction of the total number of available catalyst absorption sites occupied by NH_3 molecules. This can only take values between 0 and 1 (both inclusive).

4.2.3 Parameters

The various parameter values for pre-exponential coefficients and activation energies used in the Arrhenius rate equations are listed in Table 4.2. These parameters

were obtained from the work by Jain [10] that utilized the nonlinear greybox parameter estimation tool in MATLAB.

Table 4.2. Parameters used for simulation of the Urea-SCR system with the three-state model

Parameter	**Value**
V (m^3)	0.0037
A_{SCR} (1/mol-sec)	9.5×10^8
E_{SCR} (J/mol)	8.51×10^4
A_{ads} (1/mol-sec)	10.6652
E_{ads} (J/mol)	0.0631
A_{des} (1/sec)	6.76×10^9
E_{des} (J/mol)	1.13×10^5
A_{oxi} (1/sec)	3.501×10^{11}
E_{oxi} (J/mol)	1.523×10^5
S_1 (moles)	2.0283×10^4
S_2	0.0188
R (J/mol-K)	8.314

4.2.4 Validation

The SCR model is simulated over multiple drivecycles. The results from simulation are compared to the experimental measurements, obtained by testing the EcoCAR2 on the dynamometer, in Figures 4.3(c) and 4.3(d). Figures 4.3(a) and 4.3(b) contain the inputs to the three-state SCR model. It can be observed from the plots that the experimental measurements of NH_3 slip and NOx-out are higher than the values from simulation. This can be attributed to two reasons: (i) The NOx sensor is cross-sensitive to NH_3 present in the exhaust stream, which is why we

see a larger difference between NOx measured downstream of the catalyst and the NOx values from simulation in regions of high NH_3 slip, and (ii) The SCR system may have undergone aging over time as it has been subjected to high temperature and moisture conditions over thousands of miles on the dynamometer. The primary goal of the current project is not to obtain a very precise model, but to have one that is qualitatively similar and would allow us to test various control strategies in simulation.

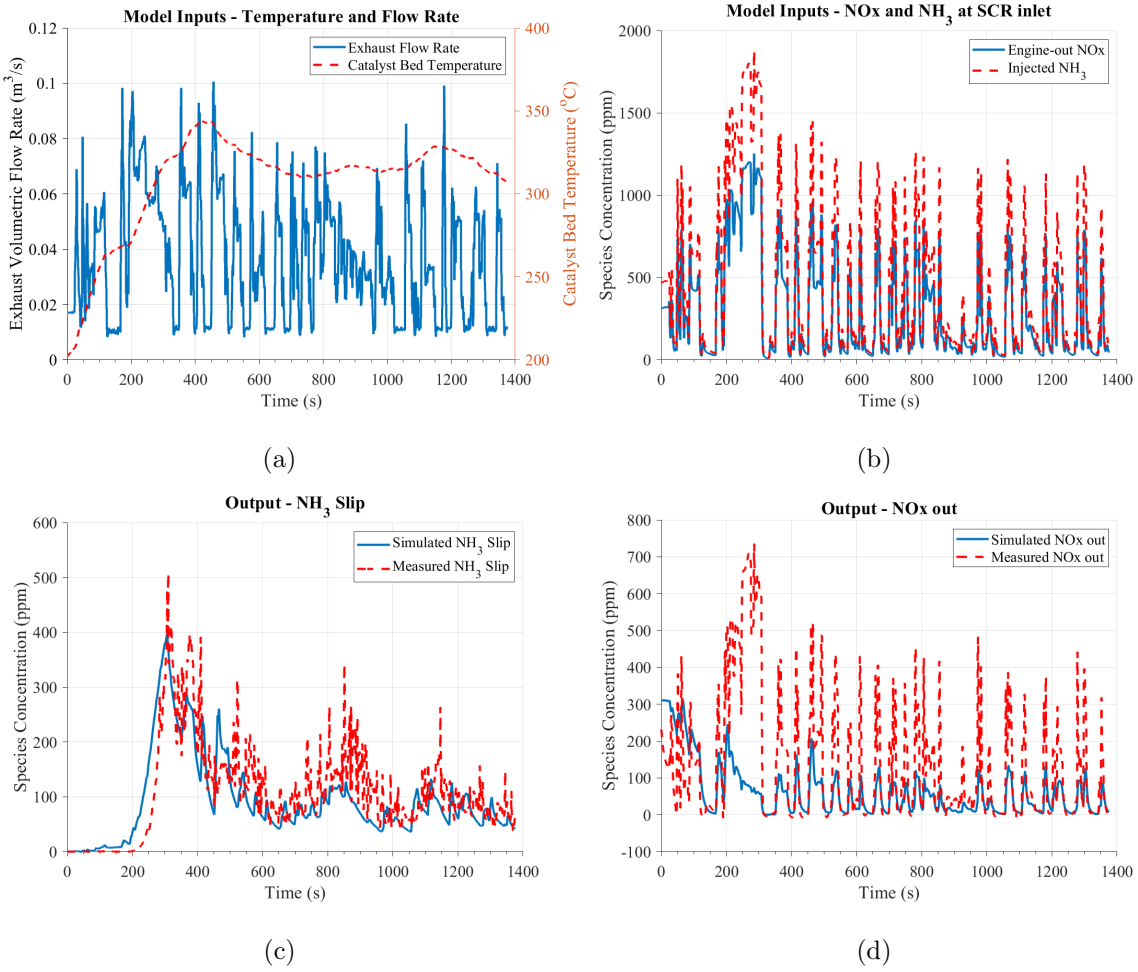

Figure 4.3. The four input signals and the two output signals of the three-state model. Plots of (a) Catalyst Bed Temperature and Exhaust Flow Rate, (b) Engine-out NOx and Injected NH_3, (c) Simulated and Measured NH_3 slip, and (d) Simulated and Measured NOx out.

5. CONTROLLER DESIGN

The Urea-SCR system enables us to maintain NOx levels within the limits specified by regulations, by dosing DEF. However, dosing a very high amount of DEF injection would lead to excessive tailpipe NH_3 slip, while dosing too little DEF would lead to excessive tailpipe NOx emissions. Further, the disturbances in an automotive system are often highly transient, which eliminates the ability to use an open-loop control algorithm. This motivates the need to employ a real-time closed-loop dosing controller. This chapter discusses the design of model-based urea dosing control algorithms and their evolution over design iterations. The control objective is laid out in Section 5.1. In Section 5.2, a model-based controller that uses inverted plant dynamics is discussed. In Section 5.3, a switched-mode controller that uses temperature to decide the operating mode is discussed. A modified and improved version of this switched-mode controller, with lookup-table-based predictive capabilities, is discussed in Section 5.4. The robustness of this controller to various control algorithm stressors are also discussed.

5.1 Control Objective

The objective of the present study is to design a urea-dosing controller that achieves the maximum possible tailpipe deNOx while keeping the tailpipe NH_3 slip under a strict upper limit. The controller needs to work well for multiple drivecycles without using apriori knowledge of the drivecycle. For this project, an allowable ceiling of 50 ppm is used. Further, the controller is to be designed using feedback from only the tailpipe NH_3 sensor.

The deNOx ability of the SCR system increases with increasing NH_3 slip. This is because an increase in tailpipe slip is generally due to an increased availability

of stored NH_3 in the catalyst. Due to this trade-off between tailpipe NH_3 slip and tailpipe NOx, the control objective is rephrased to the following: maximize tailpipe NH_3 slip while keeping it under 50 ppm.

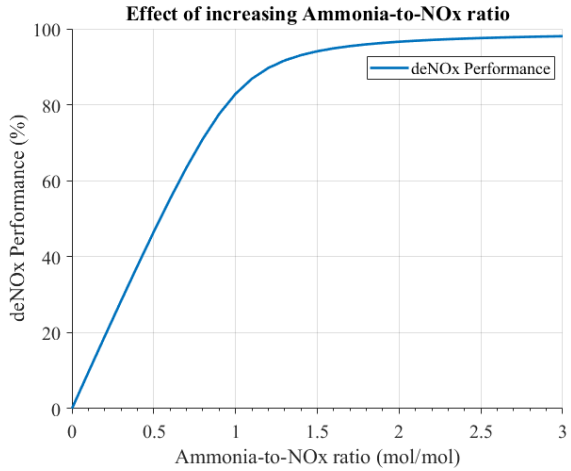

(a)

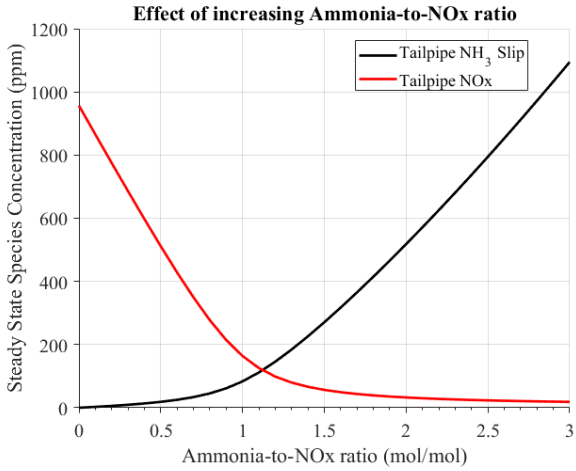

(b)

Figure 5.1. The effect of increasing the dosed Ammonia-to-NOx ratio on (a) steady-state deNOx performance and (b) steady-state tailpipe NOx and NH_3 slip obtained from steady-state simulation. Simulation operating conditions: Catalyst Bed Temperature = 310° C, Flow Rate = 0.05 m^3/s, Engine-out NOx concentration = 0.02 mol/m^3. The trade-off between the tailpipe NOx and tailpipe NH_3 slip can be clearly observed.

Many sources in the literature ([11–18]) state that their control objective is to minimize both tailpipe NOx and NH_3 slip. Such a goal would be unrealistic because in general when one of these quantities is decreased, the other increases. This trade-off is illustrated in Figure 5.1(b).

5.2 Controller-1: Model-Based + Feedback Slip-Reference Controller

Figure 5.2 illustrates the layout of the proposed controller. It consists of two major components. The first component is derived from the knowledge of the first-principle physics of the Urea-SCR system. This component is referred to as the 'Model-Based Component' for the rest of this chapter. The second component of the controller is feedback-based and is a variant of a Proportional-Integral-Derivative (PID) controller to account for undesirable attributes such as model uncertainty, dosing errors, etc. This will be referred to as the 'Feedback Component'.

5.2.1 Model-Based Component

Since the controller needs to work well on multiple drivecycles that have drastically different operating conditions of temperature range, incoming NOx concentration and flow rates, having a Model-Based Component is preferred over having a PID variant in isolation. A PID variant in isolation would require excessive tuning to ensure that it results in satisfactory performance across a wide spectrum of operating conditions. Further, this tuning effort would need to be redone periodically as the SCR system ages. In addition, a PID controller in isolation would need to be assigned relatively high gains, which may cost us the stability of the system. These problems are mitigated by using a first-principles physics-based control law. A schematic of the Model-Based Component is shown in Figure 5.3. Consider the three-state system dynamic equation of the Urea-SCR plant:

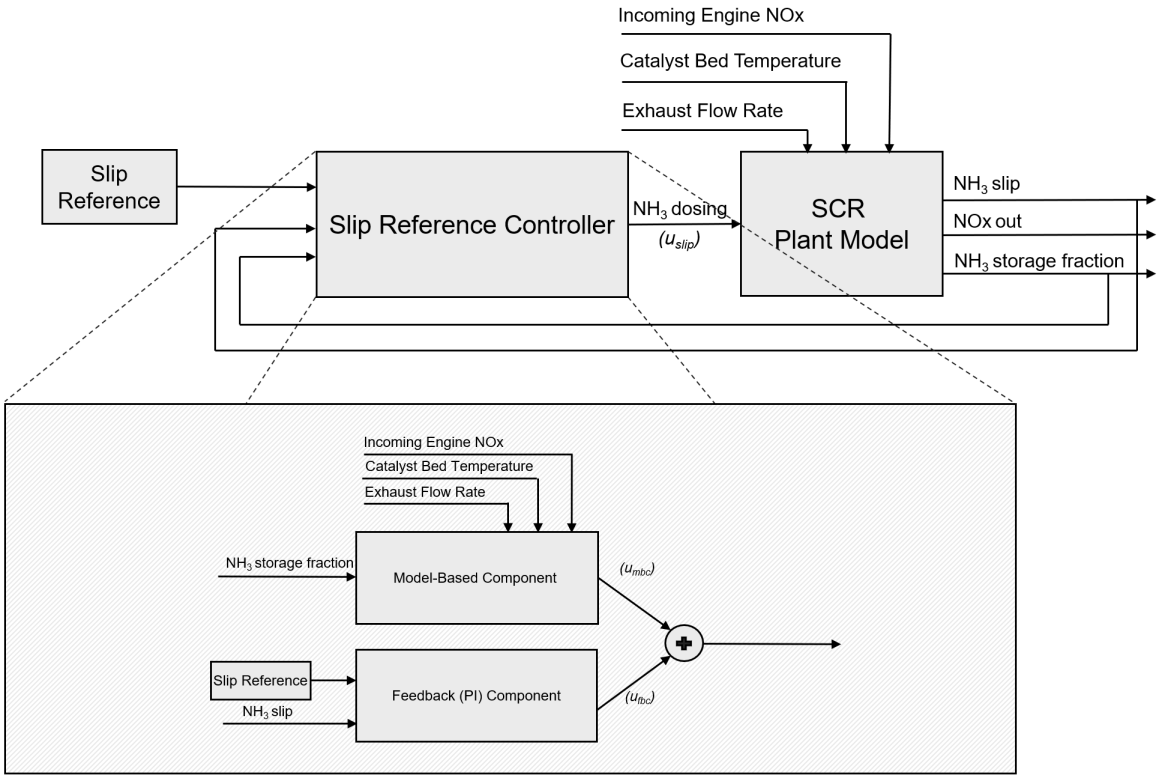

Figure 5.2. Schematic of the complete Slip-Reference Controller (Model-Based + Feedback components).

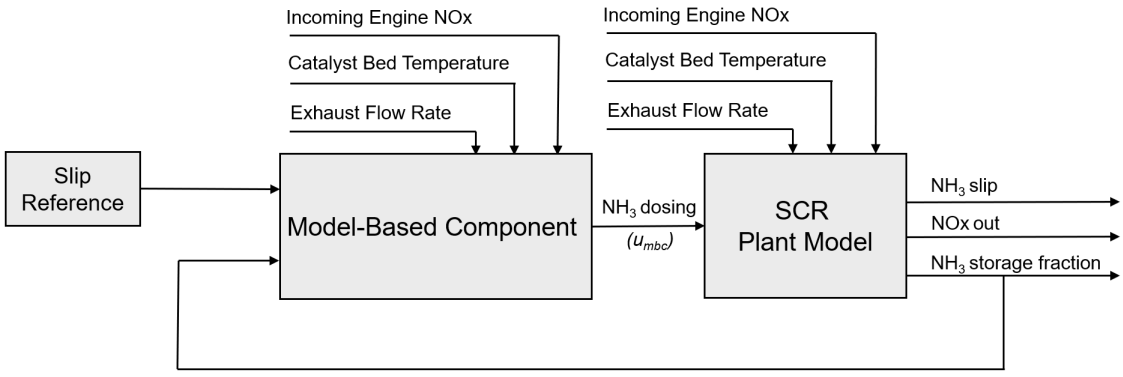

Figure 5.3. Schematic of the Model-Based component of the Slip-Reference Controller.

$$\begin{bmatrix} \dot{x}_1 \\ \dot{x}_2 \\ \dot{x}_3 \end{bmatrix} = \begin{bmatrix} \frac{F}{V}(u_1 - x_1) & 0 & -x_1(1-x_3)K & x_3K & 0 \\ \frac{F}{V}(u_2 - x_2) & -(x_2)(x_3K) & 0 & 0 & 0 \\ 0 & -(x_2)(x_3) & x_1(1-x_3) & -x_3 & -x_3 \end{bmatrix} \begin{bmatrix} 1 \\ A_{SCR}e^{\frac{-E_{SCR}}{RT}} \\ A_{ads}e^{\frac{-E_{ads}}{RT}} \\ A_{des}e^{\frac{-E_{des}}{RT}} \\ A_{oxi}e^{\frac{-E_{oxi}}{RT}} \end{bmatrix} \tag{5.1}$$

Since the current problem is one of reference tracking, we examine the state equation of the first state (x_1) in detail.

$$\dot{x}_1 = \frac{F}{V}(u_1 - x_1) - A_{ads}e^{\frac{-E_{ads}}{RT}}x_1(1-x_3)K + A_{des}e^{\frac{-E_{des}}{RT}}x_3K$$

Rearranging the terms to bring the manipulated variable (u_1) to the left hand side of the equation and all terms containing states and disturbances to the right hand side, we obtain:

$$\begin{aligned} \frac{F}{V}(u_1 - x_1) &= \dot{x}_1 + A_{ads}e^{\frac{-E_{ads}}{RT}}x_1(1-x_3)K - A_{des}e^{\frac{-E_{des}}{RT}}x_3K \\ u_1 &= x_1 + \frac{V}{F}[\dot{x}_1 + A_{ads}e^{\frac{-E_{ads}}{RT}}x_1(1-x_3)K - A_{des}e^{\frac{-E_{des}}{RT}}x_3K] \end{aligned} \tag{5.2}$$

To obtain the model-based component, we substitute $x_1 = x_{1,ref}$ because $x_{1,ref}$ is the target concentration of NH_3 slip that is to be tracked, and $\dot{x}_1 = 0$ because the controller is expected to track the slip reference fairly well. The Model-Based control law is now defined as:

$$u_{mbc} = x_{1,ref} + \frac{V}{F}[A_{ads}e^{\frac{-E_{ads}}{RT}}x_{1,ref}(1-x_3)K - A_{des}e^{\frac{-E_{des}}{RT}}x_3K] \tag{5.3}$$

where the state x_3 is the storage fraction of ammonia in the SCR catalyst. It is important for the reader to note that this Model-Based Component is not the same as a traditional feedforward control law. The difference arises from the fact that x_3, though not measurable directly, can be obtained by using a dynamic model-based observer which in turn is based on the readings obtained from the NH_3 sensor or the

NOx sensor or both, thus being able to incorporate feedback from the system. For the initial design iterations, the state x_3 is assumed to be known perfectly (without uncertainty) from the plant model. In the final control design iteration, the impact of the observer on the control performance is studied.

The Model-Based Component is implemented in Simulink. The Urea-SCR system is simulated over multiple drivecycles to evaluate the performance of the Model-Based Component, using a three-state dynamic model as the SCR plant. This would allow for fundamental errors in the controller design to be corrected. The results from these simulations are included in Figures 5.4, 5.5 and 5.6 for the UDDS, Artificial, and HWFET drivecycles, respectively. In each of these figures, the catalyst bed temperature and flow rate of exhaust gas are disturbances to the system and are plotted in subfigure (a). The control action requested (requested NH_3 dosing) by the control algorithm is shown in subfigure (b). Subfigure (c) compares the engine-out and tailpipe NOx and allows us to gauge the deNOx performance of the SCR system. Subfigure (d) contains the plot of NH_3 slip.

From Figures 5.4(d), 5.5(d) and 5.6(d) it can be observed that the controller does well to bring the Tailpipe NH_3 slip close to the reference of 50 ppm for a large portion of the drivecycle which confirms that the equation manipulation performed to obtain Equation 5.3 is correct. However, there seem to be two significant shortcomings from the controller: Firstly, there are regions in the plot that contain spikes in NH_3 Slip, which take it over the hard upper limit of 50 ppm imposed by our control objective. Secondly, in the regions where tracking of 50 ppm is done well, there always seems to be an error of 2-3 ppm which results in "waviness" of the NH_3 Slip.

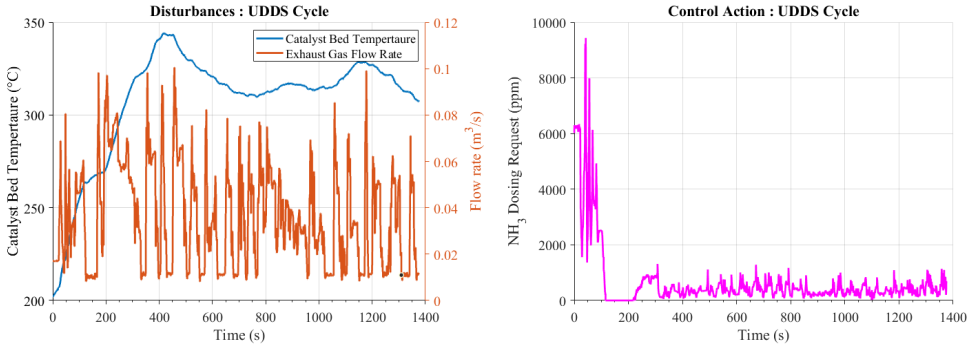

(a)

(b)

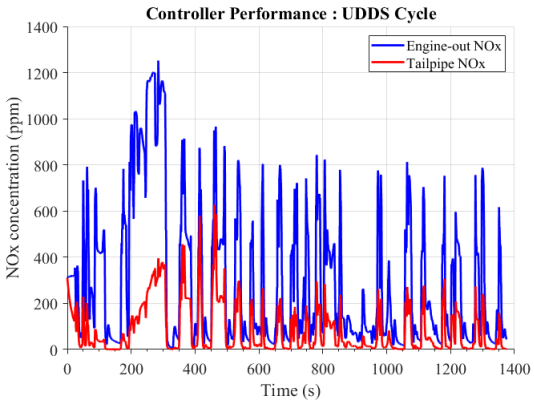

(c)

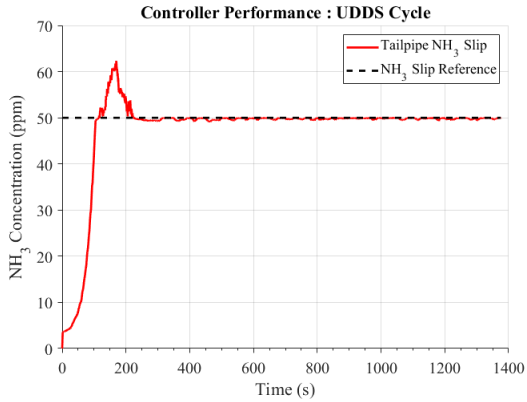

(d)

Figure 5.4. Performance of the Model-Based Component of the Slip-Reference Controller over the UDDS drivecycle with a slip-reference of 50 ppm. The plots of (a) Catalyst Bed Temperature and Exhaust Gas Flow Rate, (b) NH_3 dosing by the controller, (c) Engine-out and Tailpipe NOx, and (d) Tailpipe NH_3 Slip are shown.

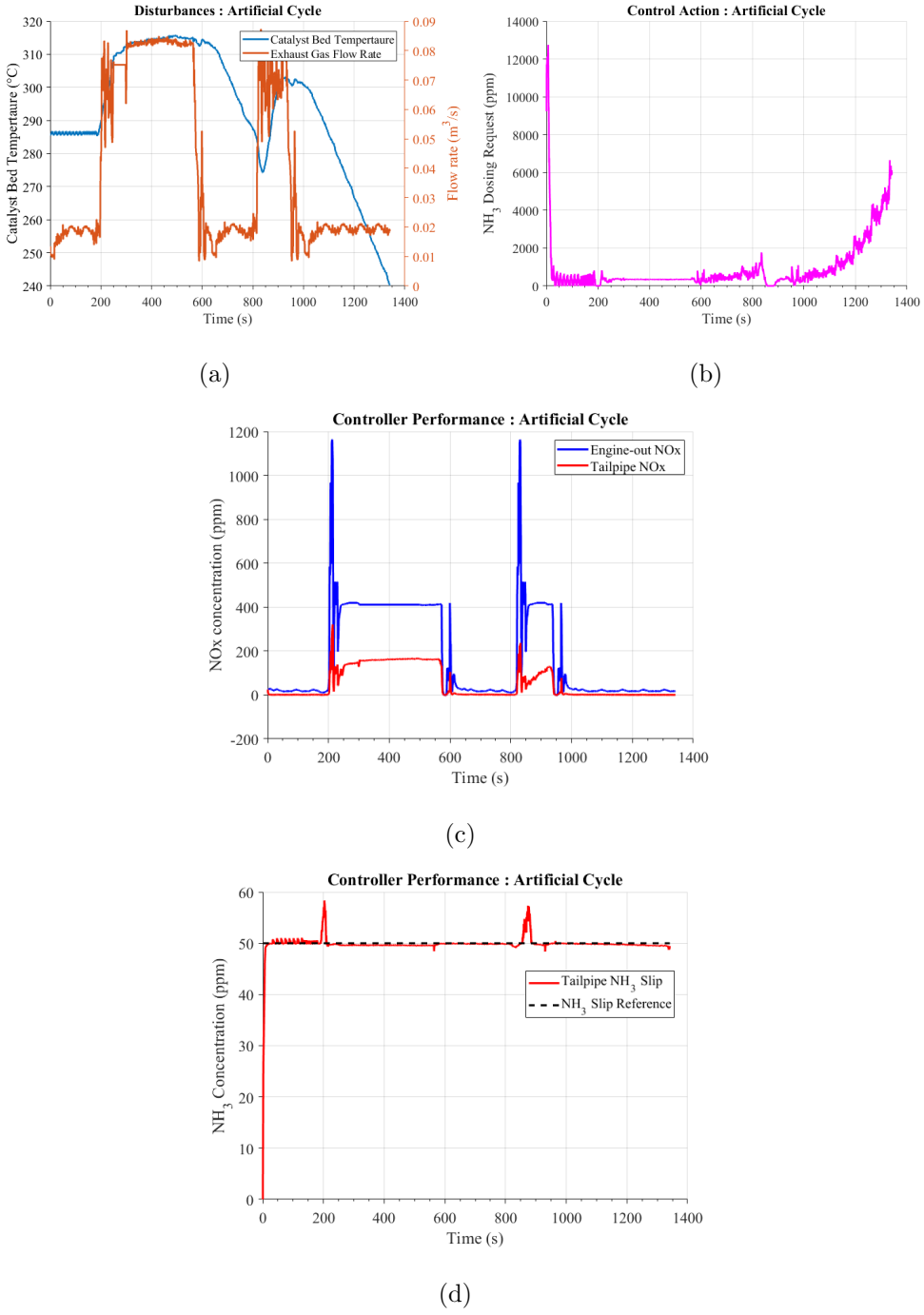

Figure 5.5. Performance of the Model-Based Component of the Slip-Reference Controller over the Artificial drivecycle with a slip-reference of 50 ppm. The plots of (a) Catalyst Bed Temperature and Exhaust Gas Flow Rate, (b) NH_3 dosing by the controller, (c) Engine-out and Tailpipe NOx, and (d) Tailpipe NH_3 Slip are shown.

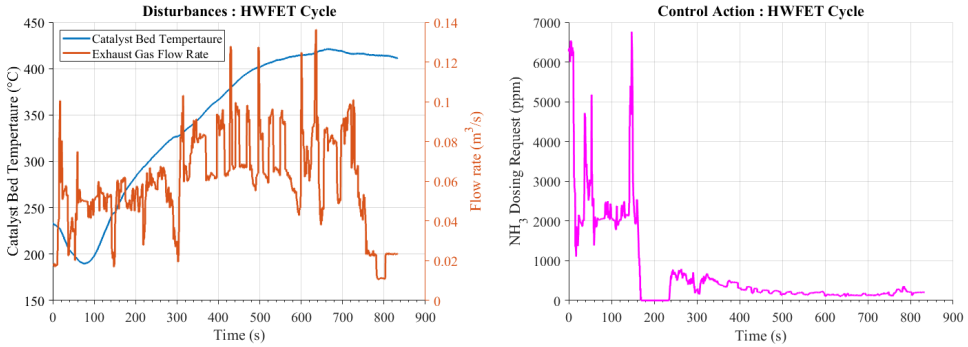

(a)

(b)

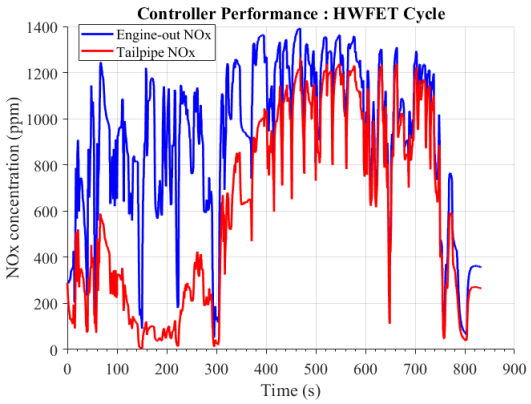

(c)

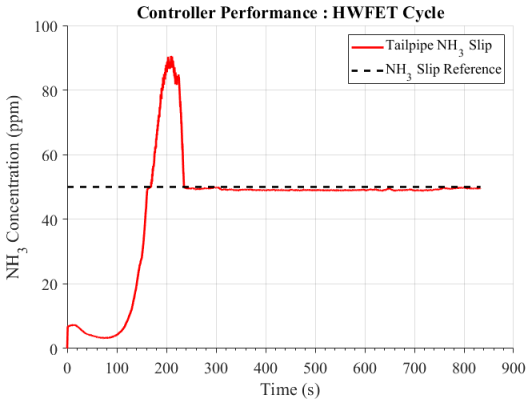

(d)

Figure 5.6. Performance of the Model-Based Component of the Slip-Reference Controller over the HWFET drivecycle with a slip-reference of 50 ppm. The plots of (a) Catalyst Bed Temperature and Exhaust Gas Flow Rate, (b) NH_3 dosing by the controller, (c) Engine-out and Tailpipe NOx, and (d) Tailpipe NH_3 Slip are shown.

5.2.2 Feedback Component

We now attempt to (i) correct the undesirable control behaviour of spikes in NH_3 slip, (ii) improve the imperfect reference tracking from "waviness", and (iii) deal with model uncertainty by adding a Feedback Component to our control algorithm. A Proportional-Integral (PI) control component is added to the system. The schematic of this Feedback component is shown in Figure 5.7. The control law for the Feedback

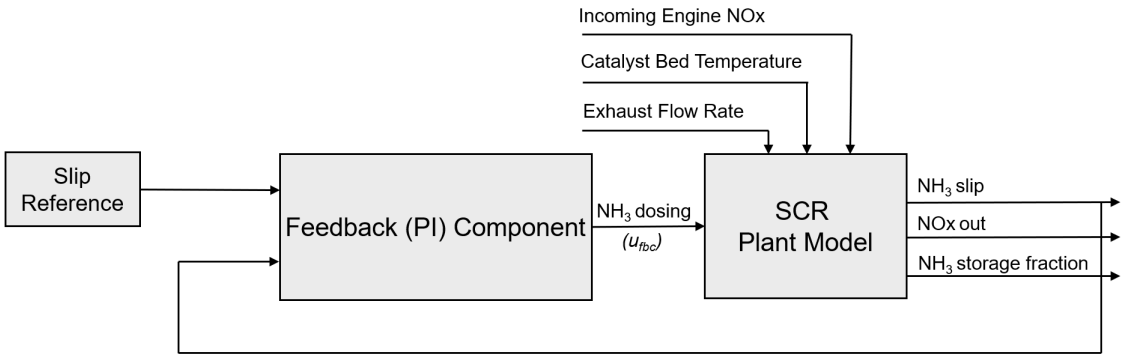

Figure 5.7. Schematic of the Feedback component of the Slip-Reference Controller.

component is given by:

$$u_{fbc} = K_{p,slip}.e_1 + K_{i,slip} \int e_1.dt \tag{5.4}$$

where $K_{p,slip}$ and $K_{i,slip}$ are the proportional and integral gains of the slip controller, respectively, and e_1 is the error in the NH_3 slip tracking given by $e_1 = x_{1,ref} - x_1$.

The complete slip-reference control law is now given by:

$$u_{slip} = u_{mbc} + u_{fbc}$$

$$u_{slip} = x_{1,ref} + \frac{V}{F}[A_{ads}e^{\frac{-E_{ads}}{RT}}x_{1,ref}(1-x_3)K - A_{des}e^{\frac{-E_{des}}{RT}}x_3K] + K_{p,slip}.e_1 + K_{i,slip}\int e_1.dt \tag{5.5}$$

The performance of the complete slip-reference controller is now evaluated in simulation. Figure 5.8 contains the tailpipe NH_3 slip obtained by running the complete slip-reference controller over three different drivecycles in simulation. From Figure 5.8, we observe that the performance of the complete slip-reference controller is similar to that of the model-based component in isolation. The two key differences are that (i) the peaks that occur during each of the three drivecycles are slightly exacerbated, and (ii) in the other regions of the drivecycles, the complete slip-reference controller is able to track the 50 ppm-reference better and mitigate the problem of "waviness". The tailpipe NH_3 slip signal obtained from running the Model-Based Component in isolation and the complete slip-reference controller are overlaid and zoomed-in in Figure 5.9. These differences can be observed clearly in this figure.

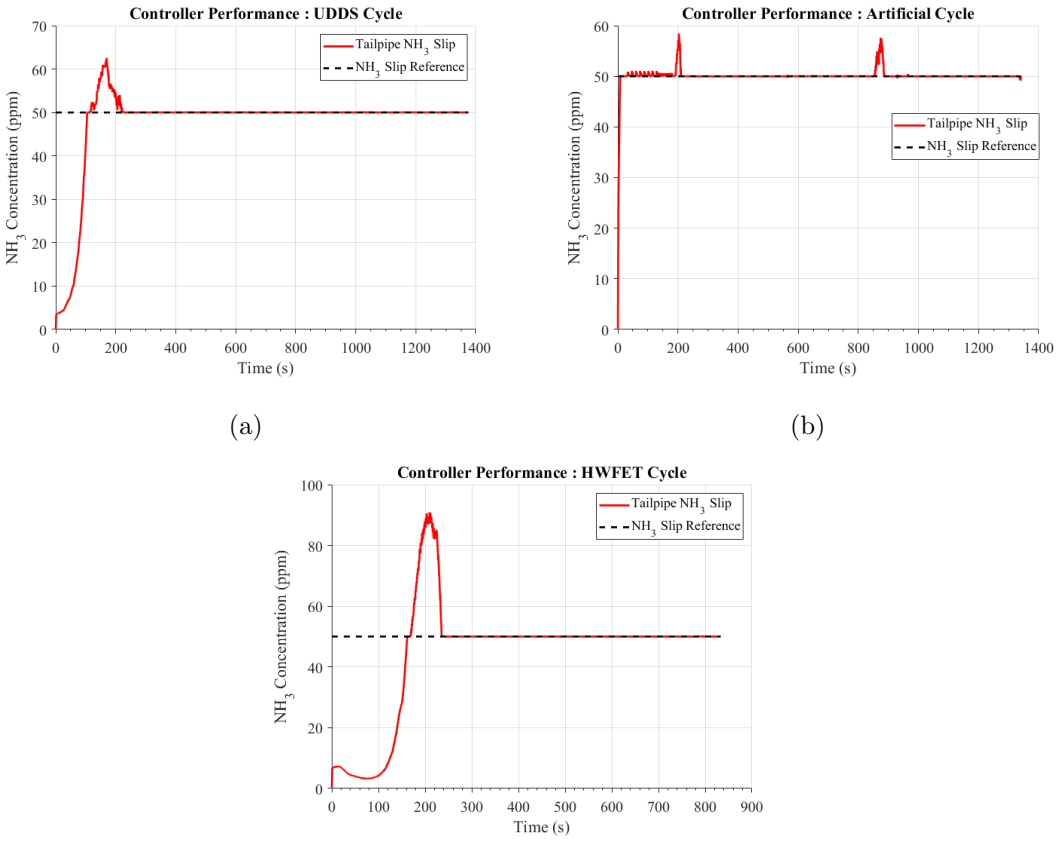

Figure 5.8. Performance of the complete slip-reference controller (Model-Based Component + Feedback component) with a slip-reference of 50 ppm. Plots of Tailpipe NH_3 Slip over the (a) UDDS, (b) Artificial, and (c) HWFET drivecycles are shown.

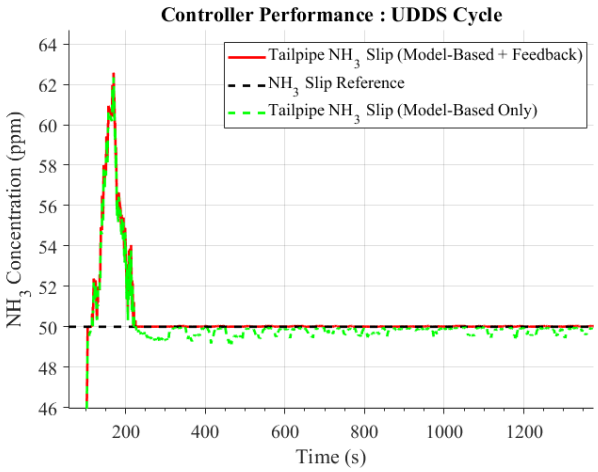

Figure 5.9. Comparison of NH_3 slip tracking performance of the Model-Based Component in isolation and the Model-Based + Feedback Controller over the UDDS cycle.

5.3 Controller-2: Switched-mode controller with Temperature-based switching

Adding a feedback component solved the problem of waviness, but the problem of peaks in NH_3 slip still needs to be addressed in order to satisfy our control objective. Careful observation of Figure 5.4 (d) shows that the peak for the UDDS cycle occurs in the region between $t = 100s$ and $t = 200s$. During this period of time Figure 5.4 (b) shows that our controller is trying to do the right thing by not dosing any NH_3 into the system. Ideally, if the controller were to have the ability to dose a "negative amount of urea", it would be possible to meet our control objective. In reality, such dosing is not possible and thus the problem of peaks requires creative control strategies. One such strategy is described in the current section.

To solve the peaks problem, we must first understand the root cause of it. At low temperatures (say <300 °C), the catalyst has a very high NH_3 storage capacity and this capacity increases exponentially with decreasing temperature. The reader may recall that the storage capacity is given by $K = S_1 e^{-S_2 T}$. Also, the net rate of ammonia adsorption is very high at these temperatures. Due to these reasons, most of the NH_3 dosed at low temperatures is adsorbed by the catalyst and very little appears as slip. Consequently, the controller needs to dose even more NH_3 in order to reach the slip reference of 50 ppm. At the moment when the 50 ppm target is reached, the catalyst now has accumulated a very large amount of NH_3 adsorbed onto itself over the time interval spent at low temperatures. If there is a considerable temperature gradient at this moment, large amounts of NH_3 would undergo desorption at once and would result in the observed peaks in NH_3 slip.

With knowledge of this behaviour we can proceed to design a control law. Since the stored ammonia is the main cause of the problem, we design a controller that works as a storage-tracking controller at low temperatures and as a slip-tracking controller otherwise. This design philosophy allows us to mitigate the probability of an NH_3 slip peak while also making available a non-zero amount of adsorbed NH_3 for NOx

reduction (as opposed to a very conservative choice of switching the controller off at low temperatures). The storage controller used is a PI controller and the control law is given by:

$$u_{storage} = K_{p,storage}.e_3 + K_{i,storage} \int e_3.dt \tag{5.6}$$

A schematic diagram of the switched mode controller is shown in Figure 5.10. The switched-mode control algorithm is given by:

$$u_{NH_3,dosing} = \begin{cases} x_{1,ref} + \frac{V}{F}[A_{ads}e^{\frac{-E_{ads}}{RT}}x_{1,ref}(1-x_3)K - A_{des}e^{\frac{-E_{des}}{RT}}x_3K \\ +K_{p,slip}.e_1 + K_{i,slip}\int e_1.dt & , T < 300\ ^oC \\ K_{p,storage}.e_3 + K_{i,storage}\int e_3.dt & , \text{otherwise} \end{cases}$$

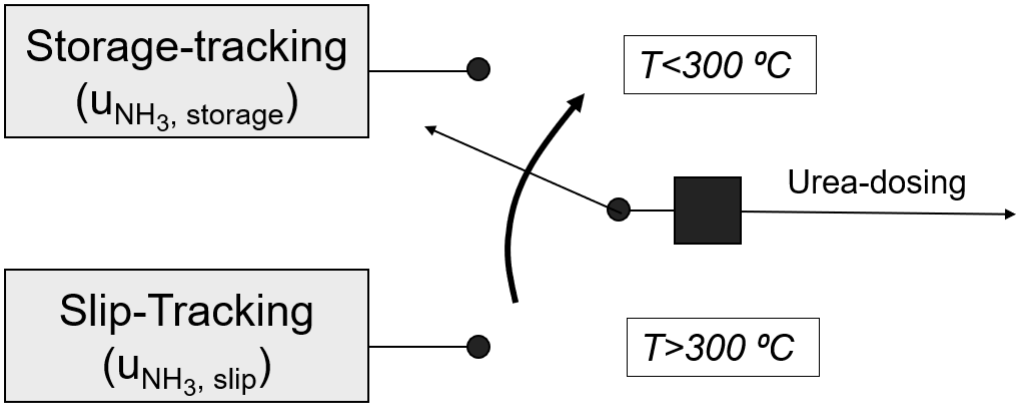

Figure 5.10. Schematic of the Switched-mode Controller.

The switched-mode control algorithm with the temperature-based switching function is then implemented in Simulink. A constant storage reference of 2% is used and a switching temperature of 300 °C is used. These values are obtained by analysing the effect of varying these quantities over multiple drivecycles. Simulations are performed over multiple drivecycles to study the effectiveness of this controller. Figures 5.11(a), 5.12(a) and 5.13(a) show how the controller changes from slip-tracking mode

to the storage-tracking mode with changes in the catalyst bed temperature. This switching clearly happens in the intended manner confirming that the switching logic is functioning correctly.Figures 5.11, 5.12 and 5.13 contain the results from simulating the Urea-SCR system over the UDDS, Artificial and HWFET drivecycles. In Figures 5.11(d), 5.11(c), 5.12(d), 5.12(c), 5.13(d) and 5.13(c) the slip and storage signals are both plotted as dashed lines when the controller is in the slip-tracking mode and are both plotted as solid lines when the controller is in storage-tracking mode. The references are plotted in green and are present only in the regions where the controller is in the corresponding mode. It can be observed that the complete switched mode controller does a good job of tracking the slip-reference and storage-reference when in the corresponding mode.

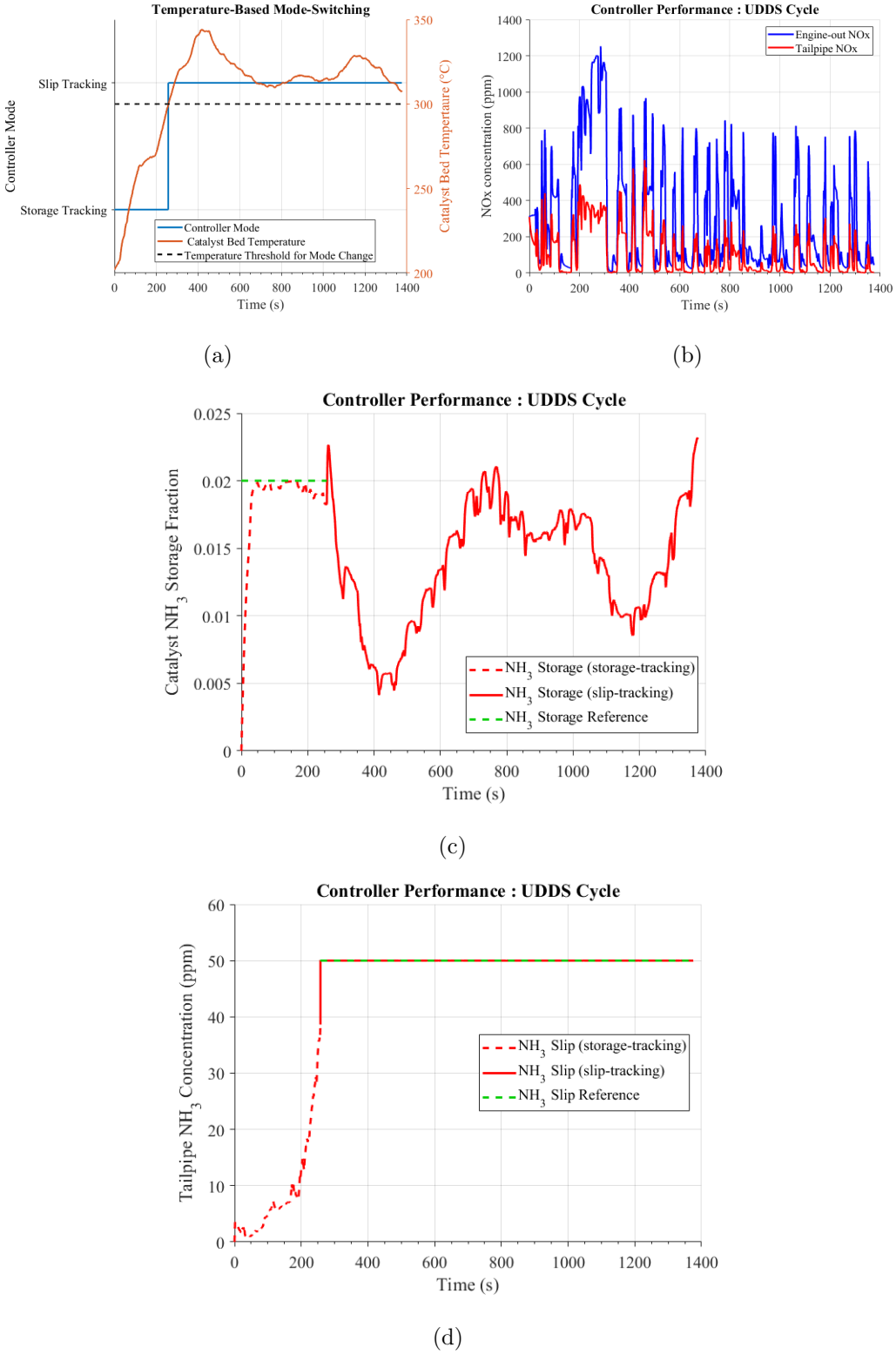

Figure 5.11. Performance of the Switched-Mode Controller over the UDDS drivecycle with a slip-reference of 50 ppm and storage-reference of 2%. The plots of (a) Catalyst Bed Temperature and Controller Mode, (b) Engine-out and Tailpipe NOx, (c) Catalyst NH_3 Storage Fraction, and (d) Tailpipe NH_3 Slip are shown.

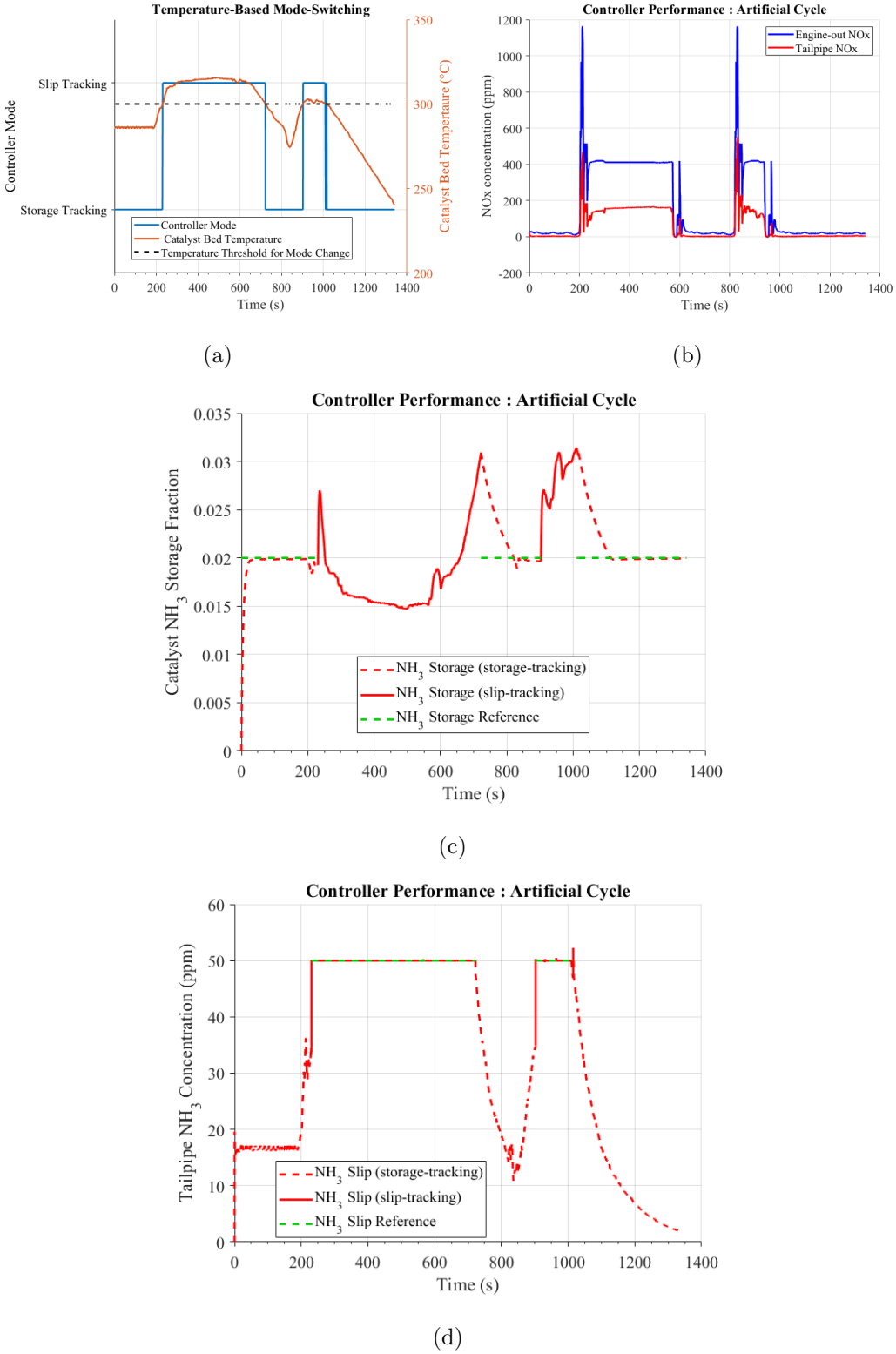

Figure 5.12. Performance of the Switched-Mode Controller over the Artificial drivecycle with a slip-reference of 50 ppm and storage-reference of 2%. The plots of (a) Catalyst Bed Temperature and Controller Mode, (b) Engine-out and Tailpipe NOx, (c) Catalyst NH_3 Storage Fraction, and (d) Tailpipe NH_3 Slip are shown.

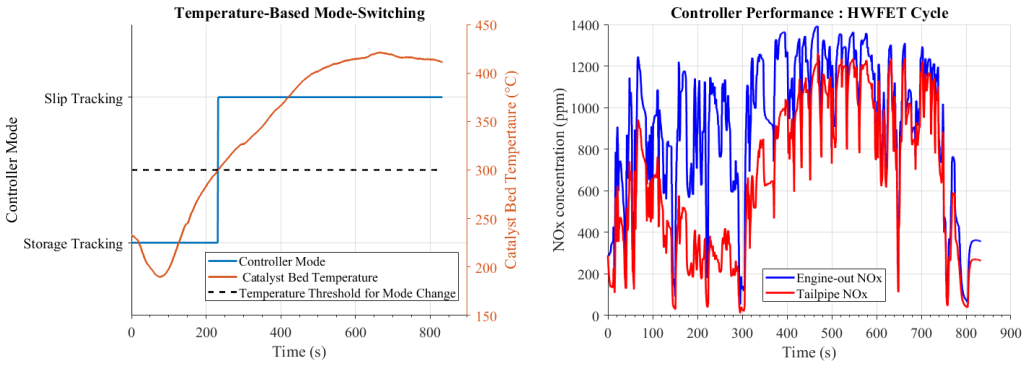

(a) (b)

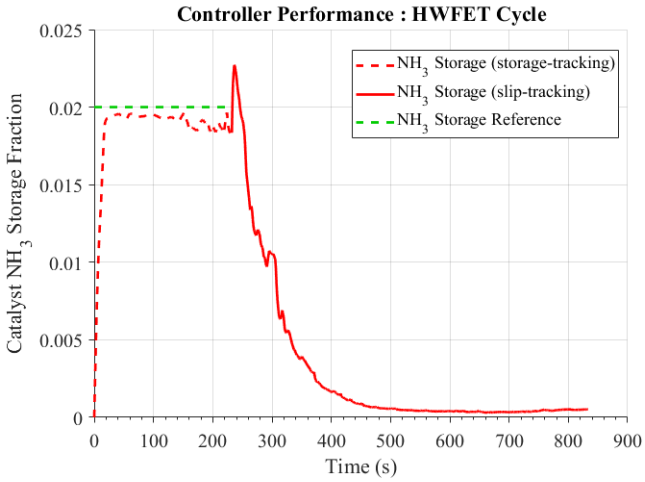

(c)

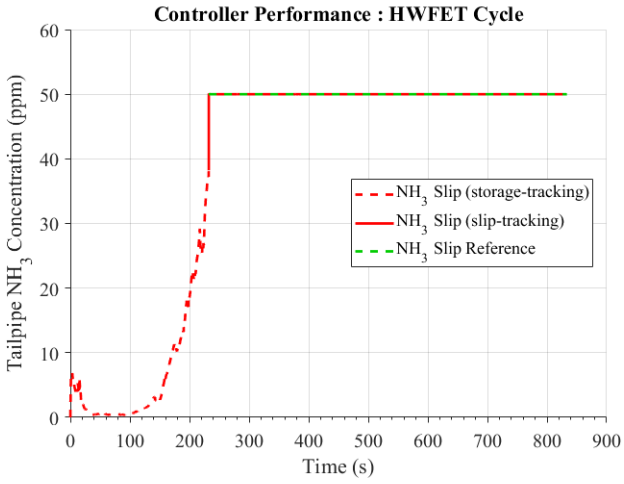

(d)

Figure 5.13. Performance of the Switched-Mode Controller over the HWFET drivecycle with a slip-reference of 50 ppm and storage-reference of 2%. The plots of (a) Catalyst Bed Temperature and Controller Mode, (b) Engine-out and Tailpipe NOx, (c) Catalyst NH_3 Storage Fraction, and (d) Tailpipe NH_3 Slip are shown.

5.4 Controller-3: Switched-mode controller based on lookup tables with Predictive Capability

While the controller proposed in the previous section satisfies the control objective, it is not aggressive enough (with NH_3 dosing because it uses a constant slip reference). We attempt to address this drawback and also reduce the number of tunables (temperature of switching) in the final control algorithm developed for the current project, which is presented in the current section. This new controller shares similarities in structure to Controller-2. The significant difference is that the storage reference is time-varying, as opposed to the static storage reference in Controller-2, and that the reference switches between various modes based on the estimate of storage and not the catalyst bed temperature.

The peaks in the NH_3 slip plots occur due to steep temperature rises that occur at low temperature conditions. In the regions where the peaks actually occur, the dosing control algorithm does the right thing of switching off dosing completely, which is the lower limit of its dosing capability. Once the slip has already gone past 50 ppm, there is not much else that can be done because of this problem of "actuator saturation".

One way to tackle this problem as a controls engineer would be to incorporate predictive control capability into the control law, in order to be able to "look ahead" into the future by simulating the model over a receding time-horizon. This train of thought would immediately lead one to think about using Model Predictive Control (MPC). While MPC is a very powerful tool to enable the controller to look into the future, it has significant drawbacks:

1. The MPC control law uses an internal optimization algorithm to come up with a set of control actions over a receding time horizon. This optimization process is computationally expensive and may require a powerful microcontroller.

2. The convergence of this optimization algorithm cannot be guaranteed for highly nonlinear systems like Urea-SCR. This problem may need work-arounds such as

bounding the run-time of the optimizer or using linearized models, which could lead to sub-optimal control performance.

3. MPC control laws have a lot of parameters that are tunable. Finding the optimal set of controller parameters requires excessive tuning effort to ensure that the controller works across a wide range of operating conditions.

To counter these problems while still ensuring "look ahead" capability, the following sequence of steps was performed:

The Urea-SCR plant model was simulated offline. Since a combination of high NH_3 storage, low temperature and a high gradient in temperature is the cause of the slip peaks, the goal of this step was to generate a multi-dimensional lookup table of the maximum allowable NH_3 storage fraction for a given set of conditions of (i) catalyst bed temperature, (ii) gradient in catalyst bed temperature, (iii) exhaust flow rates, (iv) present value of storage fraction in the catalyst, (v) present value of tailpipe NH_3 slip, and (vi) present value of incoming NOx. Taking all of these factors into account would generate a 6-D lookup table, which in theory would work well but it is not practical because we would be constrained by the upper limits on available computational power (for search/interpolation operations) and storage space on the microcontroller.

Some simplifying assumptions are made to tackle this problem: (i) The temperature gradient is set to a constant value of 1 °C/s, which is the most aggressive temperature ramp observed over multiple data sets from the testing of the car. (ii) The present value of incoming NOx was set to 0 ppm to ensure conservatism. This is because no NOx would be available for converting the stored ammonia to N_2 thus representing the worst-case scenario. (iii) Current value of slip and flowrate were observed to only weakly affect the peak slip in the window. They were set to constant values representative of the SCR system.

These assumptions leave us with catalyst bed temperature and storage. The plant was simulated offline under steady-state conditions of flow rate and NOx, but with a

temperature gradient of 1 °C/s, over a wide range of initial temperatures and storage values to observe how these two quantities affected peak slip in the 50-second window. Figure 5.14 shows how the peak slip varies with changes in storage and catalyst bed temperature. Since this plot may be difficult to read, a zoomed-in version of the same plot is presented in Figure 5.15.

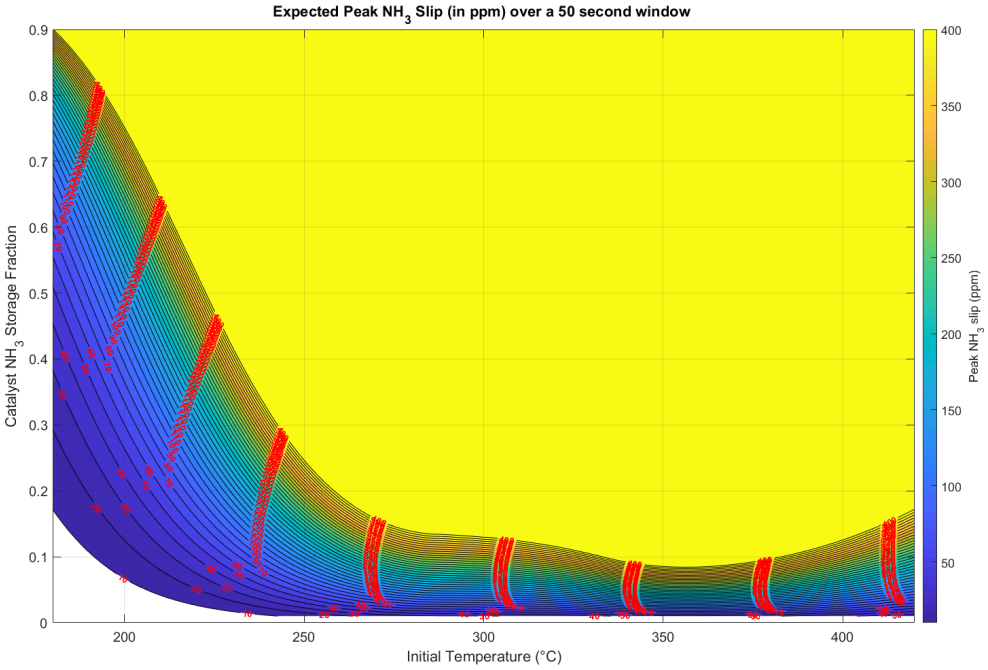

Figure 5.14. Contour plot of variation in peak NH_3 slip over a 50 second window with catalyst bed temperature and storage fraction. This was obtained by simulating the SCR system offline under steady state conditions of flow rate and NOx, but a temperature gradient of 1 °C/s

The curve corresponding to 50 ppm of peak NH_3 slip is extracted and is shown in Figure 5.16. At any given time, the storage value corresponding to the catalyst's bed temperature is used as the storage reference. We note that the values of storage reference obtained are on the order of 2-3% in the operating temperature window of the SCR system, while typical storage fraction values are on the order of 30%-60%

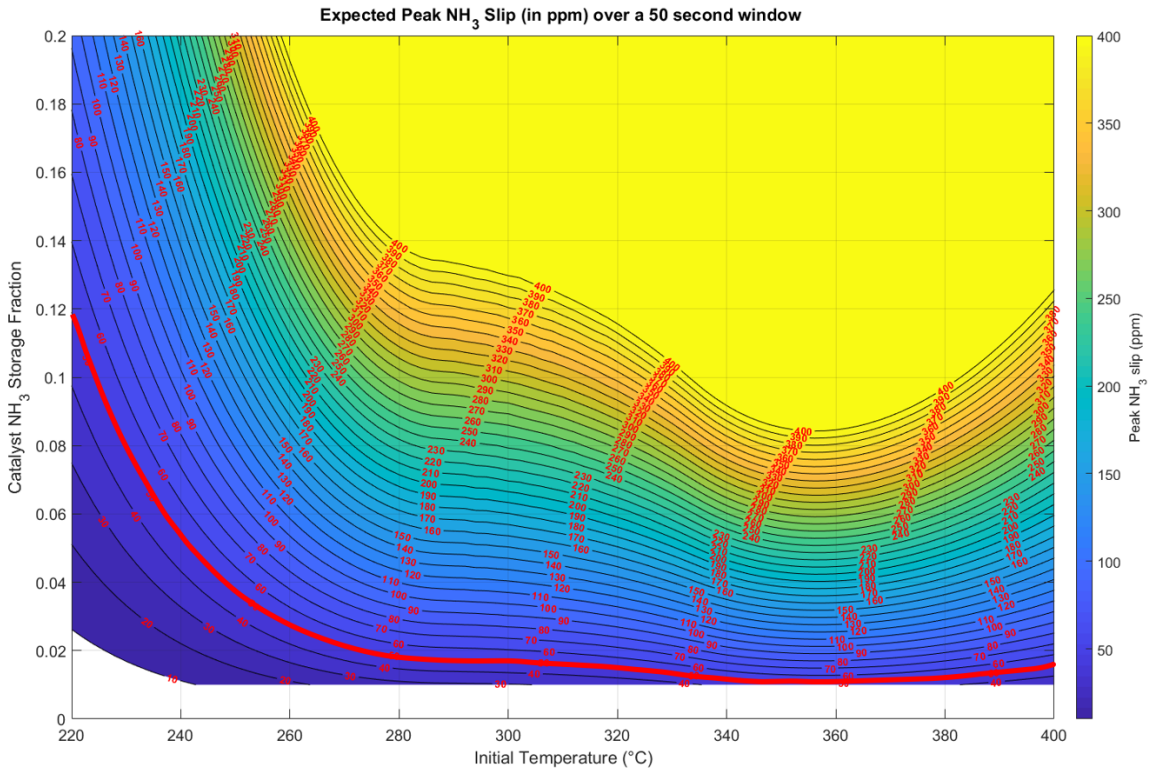

Figure 5.15. Zoomed-in view of the plot shown in Figure 5.14 to allow better visibility. The 50 ppm curve is highlighted in red. These are the ranges of temperature and storage where the SCR system is likely to operate in.

as seen in [34] and [35]. This may simply be due to the particular set of parameters being used for the SCR model in the present study and further motivates the need for a parameter set that helps to better represent the real system. Apparently, the model currently being used does not capture all of the numerical details of the actual SCR system, although we would hope that the qualitative results of this model are still relevant.

Now that we have discussed how the storage reference is created, we will look into the switching logic for the controller to decide whether to use storage-tracking or slip-tracking. At every point in time, the observed ammonia storage fraction is compared to the storage reference given by the lookup table generated from Figure

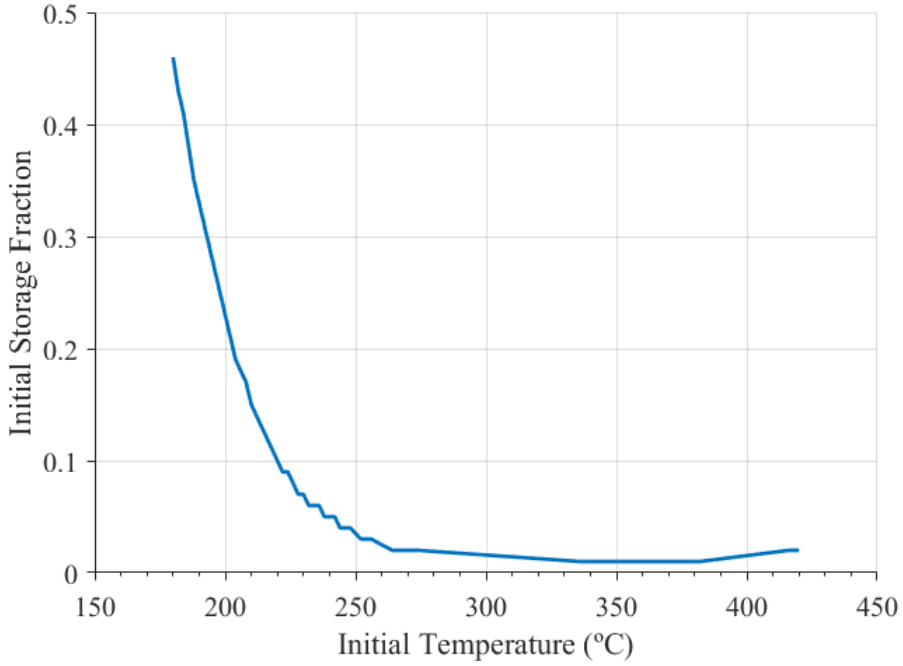

Figure 5.16. The curve corresponding to a simulated peak slip of 50 ppm in the receding 50-second time horizon. For any given temperature, there is only one corresponding storage fraction. A lookup table is formulated to contain the data points from this line.

5.16. If the observed value exceeds this reference value by a certain threshold, the controller is assigned the slip-tracking mode to ensure that NH_3 peaks do not occur in the future. In contrast, when the observed value is less than the maximum allowed value by a certain threshold (which may be different from the upper threshold), the controller is assigned the storage-tracking mode. In the case when neither of these thresholds are violated, the controller is assigned the same mode as it was in the previous time step.

Instead of using the ammonia storage fraction value (x_3) directly from the plant model, a dynamic model-based observer developed by Jain ([10]) was used to estimate the storage fraction of NH_3 in the catalyst. The estimated storage fraction of NH_3

($\hat{x}_3$) is obtained in real-time by using the following full-state feedback-based observer equations:

$$\begin{bmatrix} \dot{\hat{x}}_1 \\ \dot{\hat{x}}_2 \\ \dot{\hat{x}}_3 \end{bmatrix} = \begin{bmatrix} \frac{F}{V}(u_1 - \hat{x}_1) & 0 & -\hat{x}_1\hat{K} + x_1\hat{x}_3\hat{K} & \hat{x}_3\hat{K} & 0 \\ \frac{F}{V}(u_2 - \hat{x}_2) & -\hat{x}_2\hat{x}_3\hat{K} & 0 & 0 & 0 \\ 0 & -\hat{x}_2\hat{x}_3 & x_1 - x_1\hat{x}_3 & -\hat{x}_3 & -\hat{x}_3 \end{bmatrix} \begin{bmatrix} 1 \\ \hat{\alpha}_{SCR} \\ \hat{\alpha}_{ads} \\ \hat{\alpha}^*_{des} \\ \hat{\alpha}^*_{oxi} \end{bmatrix} + \begin{bmatrix} 0 & 0 \\ 0 & 0 \\ -\hat{K}(x_1\hat{\alpha}_{ads} + \hat{\alpha}^*_{des}) & \hat{\alpha}_{SCR}(\hat{x}_2\hat{K} + \hat{x}_3). \end{bmatrix} \begin{bmatrix} \hat{x}_1 - x_1 \\ \hat{x}_2 - (x_2 + \chi x_1) \end{bmatrix}. \tag{5.7}$$

It was observed that under ideal circumstances, when there was no parameter error and no error in the observer's initial state, the plant model output of ammonia storage fraction was exactly equal to the observer's estimate of the storage fraction.

Results from simulating this controller, with the observer incorporated in the simulations, can be seen in Figures 5.17, 5.18 and 5.19. The results were exactly identical, irrespective of whether the ammonia storage fraction was taken from the plant output or the observer's estimate of the same. It can be seen that the controller satisfies our control objective of keeping the slip close to, but under 50 ppm. It can also be seen that in the temperature ramp phases, we achieve a better tradeoff between current slip and future NH_3 peaks by using a time-varying storage reference. While the controller achieves good performance over all three drivecycles shown here, we recognize that there may be drivecycles where the performance is not as good. One potentially challenging behaviour of the control algorithm that can be noticed is the "chatter" that arises from mode changes.

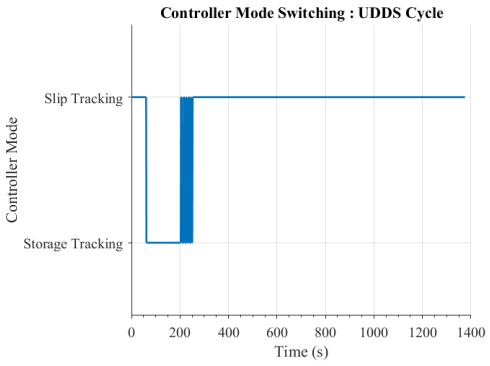

(a)

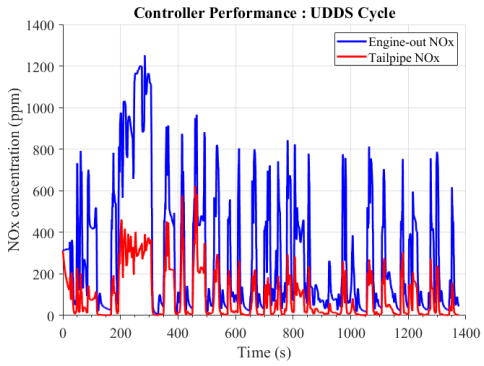

(b)

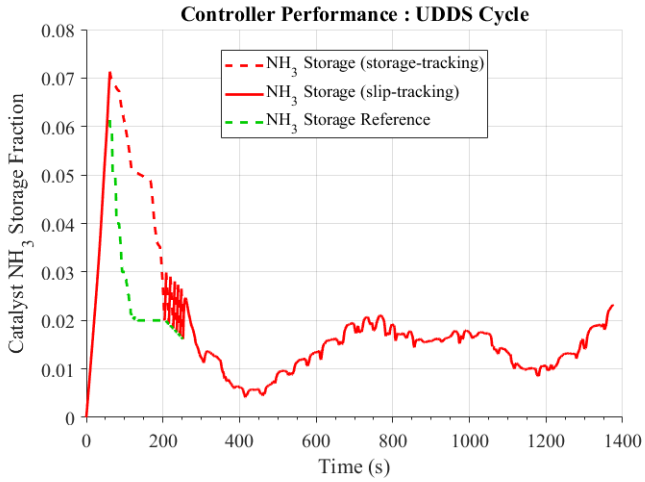

(c)

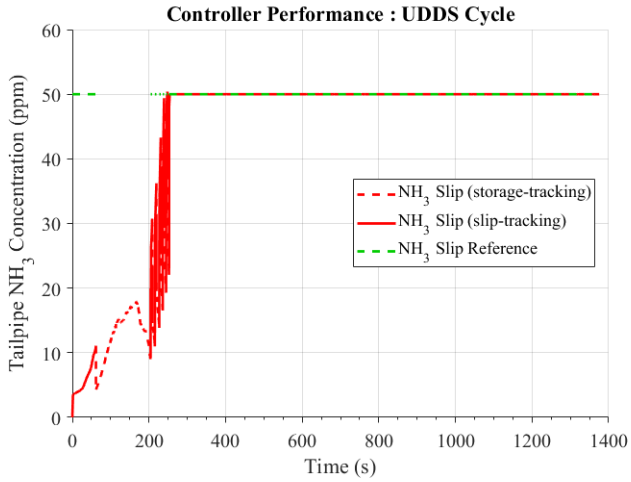

(d)

Figure 5.17. Performance of the Storage-based Switched-Mode Controller over the UDDS drivecycle with a slip-reference of 50 ppm and storage-reference of 2%. The plots of (a) Controller Mode, (b) Engine-out and Tailpipe NOx, (c) Catalyst NH_3 Storage Fraction, and (d) Tailpipe NH_3 Slip are shown.

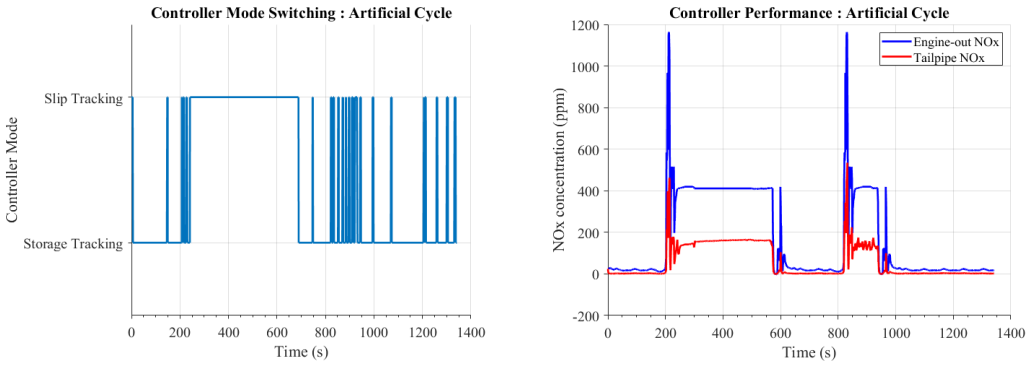

(a)

(b)

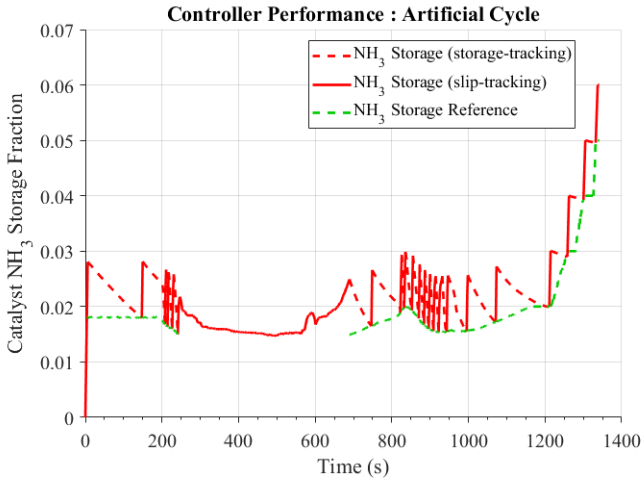

(c)

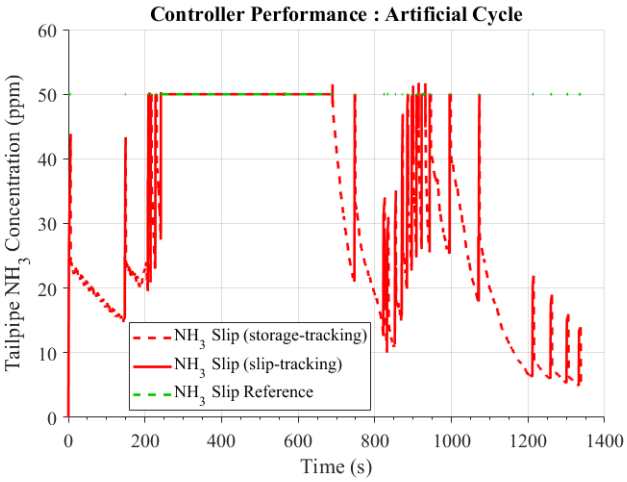

(d)

Figure 5.18. Performance of the Storage-based Switched-Mode Controller over the Artificial drivecycle with a slip-reference of 50 ppm and storage-reference of 2%. The plots of (a) Controller Mode, (b) Engine-out and Tailpipe NOx, (c) Catalyst NH_3 Storage Fraction, and (d) Tailpipe NH_3 Slip are shown.

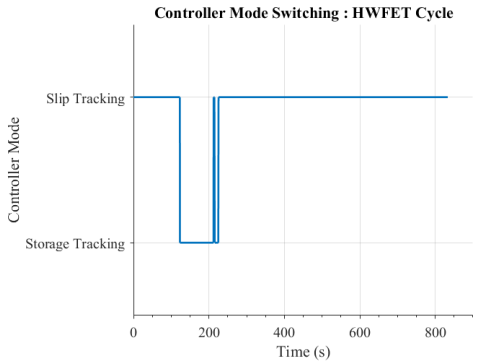

(a)

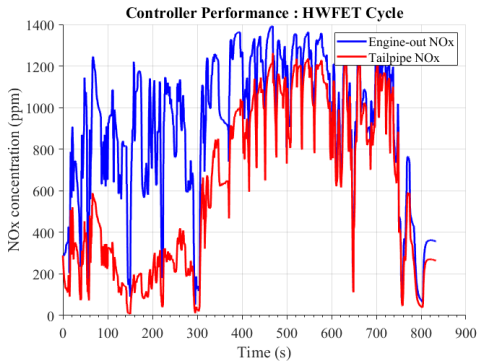

(b)

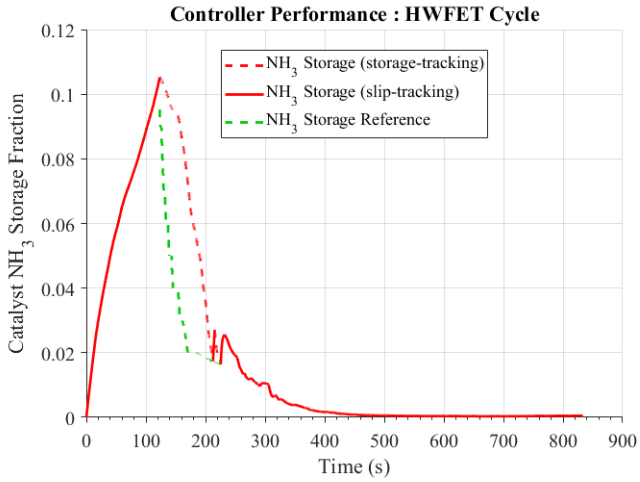

(c)

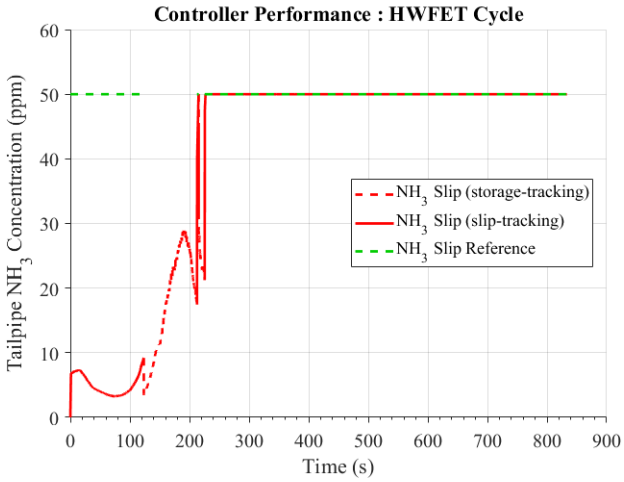

(d)

Figure 5.19. Performance of the Storage-based Switched-Mode Controller over the HWFET drivecycle with a slip-reference of 50 ppm and storage-reference of 2%. The plots of (a) Controller Mode, (b) Engine-out and Tailpipe NOx, (c) Catalyst NH_3 Storage Fraction, and (d) Tailpipe NH_3 Slip are shown.

5.4.1 Robustness Analysis

5.4.1.1 To Parameter Uncertainty in the Model

When dealing with mathematical models of systems, it is important to remember that all models are wrong, but some are useful. The parameters used in simulation studies to model the system are almost never perfectly able to replicate experimental results/observations. It is therefore necessary to study the performance of the controller by building in differences between the parameters used in the plant model and those used in the controller and/or observer. Table 5.1 lists the various combinations of errors built into the controller and observer to study the effect of parameter uncertainty on controller performance. A percentage error is added to each of the parameters in accordance with the following equation:

$$\hat{\theta} = \theta \left(1 + \frac{p_\theta}{100}\right) \tag{5.8}$$

where p_θ is the percentage error in parameter θ, which can be $K, \alpha_{SCR}, \alpha_{ads}, \alpha_{des}$, or α_{oxi}. Note that the same errors in parameters will need to be built into both the observer and the controller because these are both manipulatable by the control algorithm designer who would use the best set of parameters available, depending on the efficacy of the system identification procedure.

Table 5.1. The various combinations of parameter errors used to study the effect of parameter uncertainty.

Condition	p_K	$p_{\alpha_{SCR}}$	$p_{\alpha_{ads}}$	$p_{\alpha_{des}}$	$p_{\alpha_{oxi}}$
no error in parameters	0	0	0	0	0
+ve error in parameters	50	80	40	70	90
-ve error in parameters	-50	-80	-40	-70	-90
+ve error in some and -ve in some parameters	-50	-80	40	70	-90

Figure 5.20 shows the ability of the controller to satisfy the requirement of maintaining the Tailpipe NH_3 slip under the ceiling of 50 ppm. The performance, however, degrades depending on the type of parameter error introduced. The performance is arguably the most sub-optimal in the case when all the parameters are overestimated.

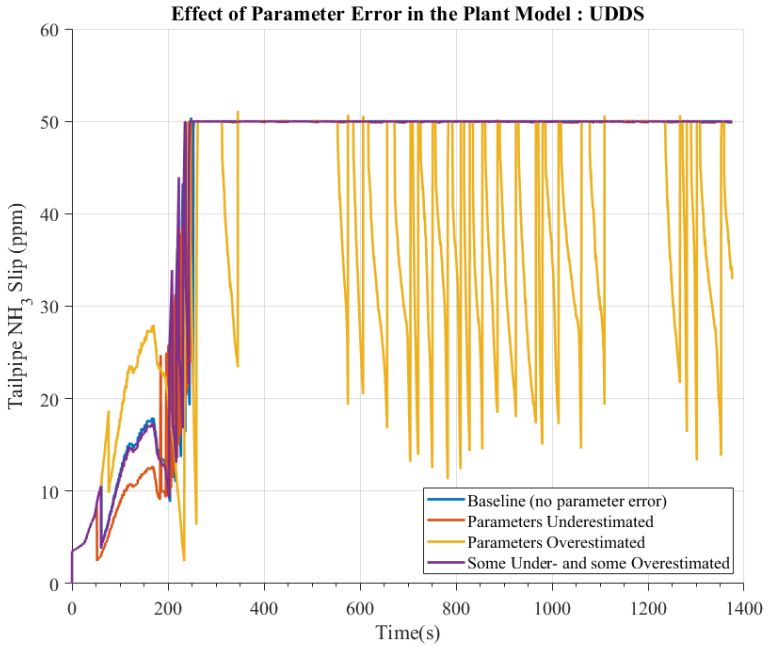

Figure 5.20. Simulation results showing the effect of parameter errors in the SCR model on controller performance over the UDDS cycle.

5.4.1.2 To Observer's Initial Estimates

The reader may recall that the controller uses information about the ammonia storage fraction value from the model-based observer. This would make the controller susceptible to estimation errors in the observer. One such error is induced by using an incorrect guess of the initial value of ammonia storage fraction in the catalyst. Storage fraction errors of 0.05 and 0.10 are built in to the initial storage guess assigned to the observer. Figure 5.21(b) shows how the observer's estimate of storage varies from the value obtained from the plant model's output. It is interesting to note that the

value of storage is overestimated in the initial phase of the drivecycle, before being underestimated and then finally converging to the plant model's output in about 200 seconds. In Figure 5.21(b) we observe that the controller is able to meet the control objective despite errors in the initial conditions of the observer.

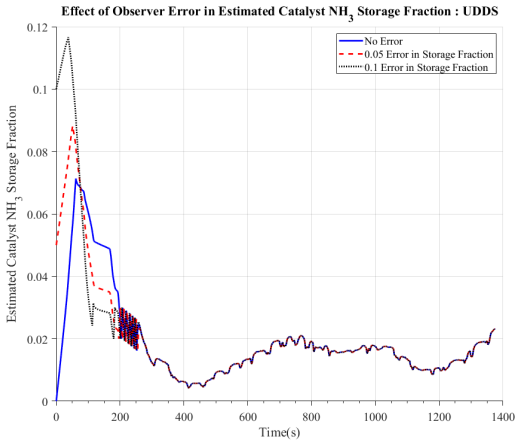

(a)

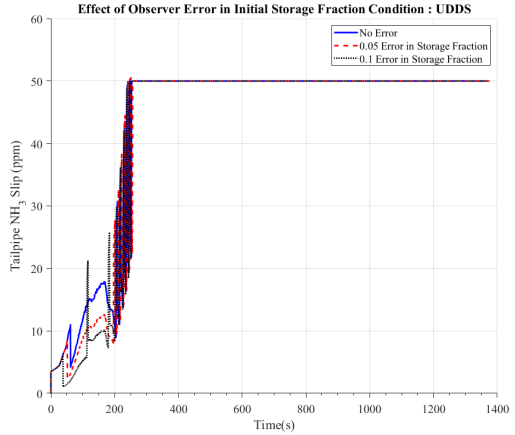

(b)

Figure 5.21. Simulation results showing the effect of errors in the observer's initial state on controller performance over the UDDS cycle. Plots of (a) estimated NH_3 storage and (b) tailipipe NH_3 slip over the drivecycle.

5.4.1.3 To Injector Faults

A common failure mode in Urea-SCR systems is that of injector faults. The injectors are subject to a wide range of temperatures and humidity, and a corrosive environment. This may lead to differences between the amount of NH_3 requested by the control algorithm and the actual amount of NH_3 dosed by the injector. To study the effects of such injector faults on controller performance, we build in dosing errors to overdose and underdose urea by 30% each. The results are plotted in Figure 5.22. We observe that the controller performs well for the UDDS and the HWFET drivecycles. Even in the Artificial drivecycle, the peak slip observed is about 52 ppm which is marginally above our specified limit.

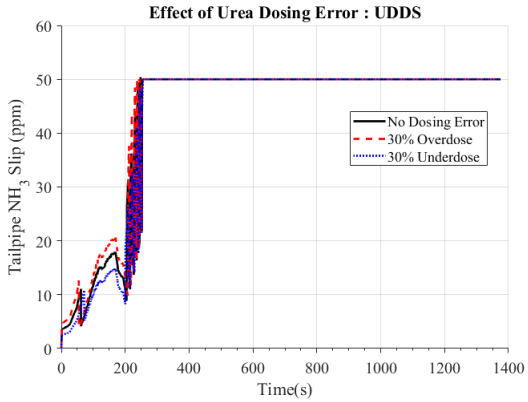

(a)

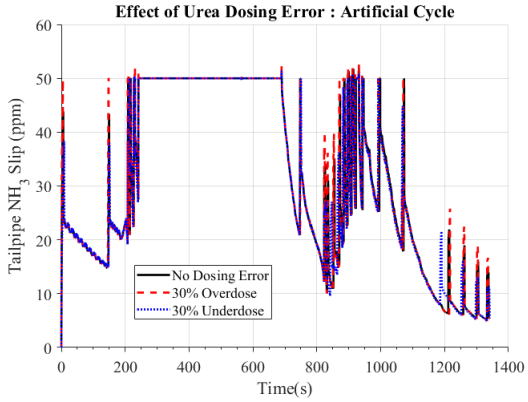

(b)

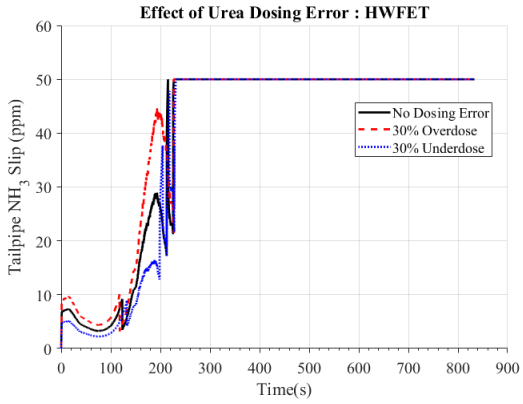

(c)

Figure 5.22. Performance of the Storage-Based Switched-Mode Controller with 30% overdosage and underdosage of urea. Plots of Tailpipe NH_3 Slip Concentration over the (a) UDDS, (b) Artificial, and (c) HWFET drivecycles.

6. CONCLUSIONS AND FUTURE WORK

6.1 Key Contributions

1. A slip-reference controller that combines a model-based component and a feedback-component was presented. This controller showed good performance when the temperature and gradient in temperature of the catalyst bed were within favourable ranges. Outside these ranges, large peaks in NH_3 slip were observed.

2. To correct for the peaks in NH_3 slip, a switched-mode controller that switches between slip-tracking and storage-tracking mode depending on the catalyst bed temperature and uses a constant storage reference was presented. While the controller satisfied the control objective, there was room for improving deNOx ability of the system.

3. To make the controller more aggressive on NH_3 dosing, a switched-mode controller that accommodates for potential peaks in NH_3 slip that could occur in the future by incorporating a time-varying storage-reference was presented. This storage reference comes from a lookup table that is generated by simulating the Urea-SCR system offline under steady-state conditions for flow rate, incoming NOx, while ramping the Temperature at a large but constant rate. Switching was performed depending on whether the estimated storage value was within the upper and lower thresholds of the storage reference. Based on results from simulation, this controller appears to be robust to uncertainty in model parameters, errors in urea dosing and error in the observer's initial conditions.

4. A lumped thermal model to simulate the catalyst brick temperature by using only the RTD upstream of the SCR catalyst was created (not included in this thesis). This model will enable potential future work of eliminating the de-

pendency on thermocouples. It also open doors to potential future projects involving engine control for aftertreatment thermal management, and integration of thermal and chemical sub-models of the SCR.

6.2 Future Work

1. A gas analyzer needs to be used to measure the tailpipe NOx concentration. This would eliminate errors caused by the cross-sensitivity of the NOx sensor to NH_3 and would enable more reliable identification of parameters.

2. A set of parameters that make the SCR model a better representation of the real SCR system needs to be identified and used in the controller, observer and SCR plant model. This would give us higher degree of confidence in the control algorithm design while testing in simulation.

3. The reason why the order of magnitude of storage fraction values is different from that found in literature needs to be investigated. This may require improving the structure of the model itself or may be solved with a better set of parameters.

4. The control strategies developed in this thesis need to be tested on high fidelity SCR models such as the four-state model developed by Jain [10], or commercially-available aftertreatment simulation software such as AVLBoost or GT-Suite.

5. The control strategies need to be validated by testing them on the real car over different drivecycles as this is the ultimate end-goal.

6. Advanced switching strategies need to be used to minimize the oscillatory nature of Controller-3 developed in this thesis. High frequency chatter could bring in dynamics of the system that are not modeled, and could potentially damage system components that are susceptible to wear and tear like the DEF injector.

7. Thermal submodels that estimate the catalyst bed temperature need to be incorporated into the control system design to eliminate the need for one or more temperature sensors. This would more accurately represent the aftertreatment system present on vehicles coming off the production line being sold to customers.

8. A Model Predictive Control (MPC) strategy needs to be developed (subject to the availability of a microcontroller with sufficient computational power) to reduce the amount of conservatism that needs to be factored into the design of the controller.

REFERENCES

REFERENCES

[1] John Conti, Paul Holtberg, Jim Diefenderfer, Angelina LaRose, James T Turnure, and Lynn Westfall. International energy outlook 2016 with projections to 2040. Technical report, USDOE Energy Information Administration (EIA), Washington, DC (United States), 2016.

[2] Rajendra K Pachauri, Myles R Allen, Vicente R Barros, John Broome, Wolfgang Cramer, Renate Christ, John A Church, Leon Clarke, Qin Dahe, Purnamita Dasgupta, et al. *Climate change 2014: synthesis report. Contribution of Working Groups I, II and III to the fifth assessment report of the Intergovernmental Panel on Climate Change*. IPCC, 2014.

[3] JB Heywood. *Internal Combustion Engine Fundamentals*. McGraw-Hill, New York, 1988.

[4] Han Hao, Yong Geng, and Joseph Sarkis. Carbon footprint of global passenger cars: Scenarios through 2050. *Energy*, 101:121–131, 2016.

[5] Lifeng Xu, William Watkins, Rachel Snow, George Graham, Robert McCabe, Christine Lambert, and RO Carter III. Laboratory and engine study of urea-related deposits in diesel urea-scr after-treatment systems. *SAE Transactions*, pages 202–209, 2007.

[6] W. Addy Majewski Hannu Jääskeläinen. *Urea Dosing Control*, 2017 (accessed April 28, 2017). https://dieselnet.com/tech/cat_scr_mobile_control.php.

[7] *Cars and Light-Duty Trucks*, 2017 (accessed April 28, 2017). https://dieselnet.com/standards/us/ld_t2.php.

[8] Jagdish Rajendra Hiremath. *Development of Urea-SCR Dosing Control Strategies for a Diesel Electric Hybrid Car*. Master's thesis, 2015.

[9] *Cars and Light-Duty Trucks-Tier 3*, 2017 (accessed April 28, 2017). https://dieselnet.com/standards/us/ld_t3.php.

[10] Kaushal Kamal Jain. *Modeling of NH_3 Storage in Vanadia-Based SCR Catalyst for Urea-Dosing Control in a Diesel-Electric Hybrid Car*. Master's thesis, Purdue University, 2017.

[11] Qingwen Song and George Zhu. Model-based closed-loop control of urea scr exhaust aftertreatment system for diesel engine. *SAE Transactions*, pages 102–110, 2002.

[12] John N Chi and Herbert FM DaCosta. Modeling and control of a urea-scr aftertreatment system. Technical report, SAE Technical Paper, 2005.

[13] Paul Tennison, Christine Lambert, and Michael Levin. NOx control development with urea scr on a diesel passenger car. *SAE transactions*, pages 573–579, 2004.

[14] Mona Meisami-Azad, Javad Mohammadpour, Karolos M Grigoriadis, and Michael P Harold. An adaptive control strategy for urea-scr aftertreatment system. In *Proceedings of the 2010 American Control Conference*, pages 3027–3032. IEEE, 2010.

[15] Ming Feng Hsieh and Junmin Wang. Staircase ammonia coverage ratio profile control for diesel engine two-cell selective catalytic reduction systems. In *Proceedings of the 2010 American control conference*, pages 3003–3008. IEEE, 2010.

[16] Tan Feng and Lin Lü. The characteristics of ammonia storage and the development of model-based control for diesel engine urea-scr system. *Journal of Industrial and Engineering Chemistry*, 28:97–109, 2015.

[17] Gillis Hommen, Frank Kupper, and Xander Seykens. Robust, model-based urea dosing control for scr aftertreatment systems using a cross-sensitive tailpipe nox sensor. Technical report, SAE Technical Paper, 2017.

[18] Jinghua Zhao, Yunfeng Hu, Xun Gong, and Hong Chen. Modelling and control of urea-scr systems through the triple-step non-linear method in consideration of time-varying parameters and reference dynamics. *Transactions of the Institute of Measurement and Control*, 40(1):287–302, 2018.

[19] Christoph M Schär, Christopher H Onder, Hans P Geering, and M Elsener. Control of a urea scr catalytic converter system for a mobile heavy duty diesel engine. *SAE transactions*, pages 1180–1188, 2003.

[20] Maruthi Devarakonda, Gordon Parker, John H Johnson, Vadim Strots, and Shyam Santhanam. Model-based estimation and control system development in a urea-scr aftertreatment system. *SAE International Journal of Fuels and Lubricants*, 1(1):646–661, 2009.

[21] Devesh Upadhyay and Michiel Van Nieuwstadt. Model based analysis and control design of a urea-scr denox aftertreatment system. 2006.

[22] Thomas L McKinley and Andrew G Alleyne. Adaptive model predictive control of an scr catalytic converter system for automotive applications. *IEEE transactions on control systems technology*, 20(6):1533–1547, 2011.

[23] Sheng Yao, Mark Shost, Joon-Ho Yoo, David Cabush, David Racine, Robert Cloudt, Frank Willems, et al. Ammonia sensor for closed-loop scr control. *SAE international journal of passenger cars-electronic and electrical systems*, 1(2008-01-0919):323–333, 2008.

[24] Abdul R Ofoli. Experimental demonstration of ammonia storage and slip modeling with control for an scr aftertreatment system. *IEEE Transactions on Industry Applications*, 50(4):2342–2348, 2014.

[25] Mu Wang. *Model-based control of selective catalytic reduction systems*. PhD thesis, 2015.

[26] Christoph M Schar, Christopher H Onder, and Hans Peter Geering. Control of an scr catalytic converter system for a mobile heavy-duty application. *IEEE Transactions on Control Systems Technology*, 14(4):641–653, 2006.

[27] Hui Zhang and Junmin Wang. Adaptive sliding-mode observer design for a selective catalytic reduction system of ground-vehicle diesel engines. *IEEE/ASME Transactions on Mechatronics*, 21(4):2027–2038, 2016.

[28] Ming-Feng Hsieh. *Control of diesel engine urea selective catalytic reduction systems*. PhD thesis, The Ohio State University, 2010.

[29] Pingen Chen and Junmin Wang. Estimation and adaptive nonlinear model predictive control of selective catalytic reduction systems in automotive applications. *Journal of Process Control*, 40:78–92, 2016.

[30] Isabella Nova and Enrico Tronconi. *Urea-SCR technology for deNOx after treatment of diesel exhausts*. Springer, 2014.

[31] Delphi. *NH3 Sensor User Manual*. 2011.

[32] Continental. *Smart NOx Sensor: Handling, Installation and Mounting guide*. 2011.

[33] Harshil Rajesh Angre. *Control of Urea Dosing for Urea SCR System in a Diesel-powered Vehicle*. Master's thesis, Purdue University, 2018.

[34] Jinghua Zhao, Zhigang Chen, Yunfeng Hu, and Hong Chen. Urea-scr process control for diesel engine using feedforward-feedback nonlinear method. *IFAC-PapersOnLine*, 48(8):367–372, 2015.

[35] Hisao Haga, Hiroyuki Kojima, Naoko Fukushi, Naoki Ohya, and Takuya Mito. Optimized nh3 storage control for next generation urea-scr system. Technical report, SAE Technical Paper, 2015.